WISC-MILW-94-TH-18

CBR Anisotropy from Primordial Gravitational Waves in Two-component Inflationary Cosmology

Scott Koranda
Department of Physics, University of Wisconsin – Milwaukee
P.O. Box 413, Milwaukee, Wisconsin 53201, U.S.A.
email: skoranda@dirac.phys.uwm.edu

Bruce Allen
Department of Physics, University of Wisconsin – Milwaukee
P.O. Box 413, Milwaukee, Wisconsin 53201, U.S.A.
email: ballen@dirac.phys.uwm.edu
(February 5, 2008)

Abstract

We examine stochastic temperature fluctuations of the cosmic background radiation (CBR) arising via the Sachs-Wolfe effect from gravitational wave perturbations produced in the early universe. We consider spatially flat, perturbed FRW models that begin with an inflationary phase, followed by a mixed phase containing both radiation and dust. The scale factor during the mixed phase takes the form $a(\eta) = c_1\eta^2 + c_2\eta + c_3$, where c_i are constants. During the mixed phase the universe smoothly transforms from being radiation to dust dominated. We find analytic expressions for the graviton mode function during the mixed phase in terms of spheroidal wave functions. This mode function is used to find an analytic expression for the multipole moments $\langle a_l^2 \rangle$ of the two-point angular correlation function $C(\gamma)$ for the CBR anisotropy. The analytic expression for the multipole moments is written in terms of two integrals, which are evaluated numerically. The results are compared to multipoles calculated for models that are *completely* dust dominated at last-scattering. We find that the multipoles $\langle a_l^2 \rangle$ of the CBR temperature perturbations for $l > 10$ are significantly larger for a universe that contains both radiation and dust at last-scattering. We compare our results with recent, similar numerical work and find good agreement. The spheroidal wave functions may have applications to other problems of cosmological interest.

PACS numbers: 98.80.Cq, 98.80.C, 98.80.Es

I. INTRODUCTION

This paper considers the effect of primordial gravitational waves on the cosmic background radiation (CBR). We consider spatially flat, perturbed Friedman-Robertson-Walker (FRW) universes that begin with an early inflationary phase. As the universe rapidly expands, perturbations of the spatial geometry that are local in origin (eg. thermal fluctuations) are quickly redshifted both in amplitude and wavelength. After sufficient inflation these perturbations are no longer visible to an observer; the only perturbations that remain visible within a Hubble sphere are quantum-mechanical zero-point fluctuations. Because these perturbations extend to arbitrarily high frequencies they can not be redshifted away. Since the only significant perturbations remaining after inflation are zero-point fluctuations, we assume that the initial state of the universe was the vacuum state appropriate to de Sitter space, containing only the quantum fluctuations and no additional excitations. As the universe continues to expand after inflation, these quantum fluctuations are redshifted to longer wavelengths and amplified; one may think of this in terms of particle (graviton) production (as we do), non-adiabatic amplification, or super-radiant scattering. In the present epoch the occupation numbers of the graviton modes are large. This is not surprising. It has been shown that one may treat the collective effects of primordial gravitational waves as being due to the presence of a stochastic background of classical gravitational waves, and since gravitons are bosons, such an interpretation is only possible if the occupation numbers are large.

Sachs and Wolfe [1] showed how gravitational wave perturbations result in CBR temperature anisotropy. As photons from the CBR propagate, the paths they follow are perturbed by the metric perturbation h_{ij}, which in this discussion is due entirely to primordial gravitational waves. The energies of the photons are perturbed, which results in temperature fluctuations from point to point on the celestial sphere. These temperature fluctuations are usually characterized by the two-point angular correlation function $C(\gamma)$ defined on the celestial sphere. Here γ is the angle between two points on the sphere. Most often the two-point angular correlation function is expanded in terms of Legendre polynomials, and the expansion coefficients or multipole moments are calculated. For a derivation of the angular correlation function for spatially flat cosmologies see the recent paper by Allen and Koranda [2]. Henceforth we will assume that the reader is familiar with this paper, which contains a detailed review of previous work on this problem, a comprehensive discussion of the physical motivation, and a detailed and self-contained "first-principles" calculation.

Early work on this subject [3,4,5,6] assumed that the universe was completely dust dominated at last-scattering when the CBR decoupled, as did recent work by White [7] which presented a concise derivation of the formula for the multipole moments due to tensor perturbations. Also recently, Grishchuk has adapted the terminology and techniques of quantum optics to the analysis [8]. Grishchuk stresses the importance of the phase correlations between the modes of the metric perturbations. A similar analysis by Allen and Koranda [2] using standard "quantum field theory in curved space" techniques found equivalent results. We also showed that the now standard formula given by Abbott and Wise [5] and Starobinsky [6] for the l'th multipole moment is a long wavelength approximation to an exact formula. Both the work by Grishchuk, and by Allen and Koranda assumed that the universe was completely dust dominated at last-scattering.

The first authors to consider the CBR anisotropy (within the framework of the Sachs-Wolfe effect) for a universe that was *not* completely dust dominated at last-scattering were Turner, White, and Lidsey [9]. They used a "transfer function" to express the solutions of the wave equation for the gravitational wave amplitude in terms of the standard long wavelength formula given by Abbott and Wise. They found that the standard formula, which assumes that the universe is *completely* dust dominated at last-scattering, consistently underestimates the contribution of gravitational waves to the CBR anisotropy. More recent work by Ng and Speliotopoulos [10] used numerical methods to integrate the wave equation and found similar results. Neither of these studies used analytic expressions for the gravitational wave amplitude (or equivalently, the graviton mode function).

Other work has been done which does not directly use the Sachs-Wolfe formula to calculate the anisotropy due to gravitational waves. Crittenden et. al. [11] numerically evolved the photon distribution function using first-order perturbation theory of the general relativistic Boltzmann equation for radiative transfer, and included a Thomson scattering source term. Dodelson, Knox and Kolb [12] have done a similar numerical analysis. Both found that the standard formula of Abbott and Wise is only accurate for small l multipole moments, and consistently underestimates the contribution of the gravitational waves to the CBR anisotropy for higher l moments.

In this paper we give the first correct analytic expression for the graviton mode function in a cosmology that transforms smoothly from being radiation to dust dominated. (We correct a minor error in earlier work by Sahni [13] and Nariai [14] which claimed to find an analytic expression for the mode function.) We use this analytic expression and the Sachs-Wolfe formula to find an analytic expression for the multipole moments $\langle a_l^2 \rangle$ of the angular correlation function $C(\gamma)$. The analytic expression for the multipole moments is written in terms of two integrals; we use numerical methods to evaluate these integrals and report numerical values for the multipole moments. We compare our results with those mentioned above, and find good agreement.

The paper is organized as follows. In section II we reproduce general expressions for the angular correlation function derived in [2], and explain how one uses these formulae to calculate the multipole moments for any spatially flat, inflationary cosmological model. In section III we introduce our cosmological model, which "begins" with an infinite de Sitter phase followed by a mixed phase that contains both radiation and dust. Early in the mixed phase the universe is radiation dominated; later it transforms smoothly from being radiation dominated to dust dominated. In section IV we solve the massless Klein-Gordon equation (or wave equation) for the graviton mode function. During the mixed phase the solutions to the wave equation are expressed in terms of spheroidal wave functions. The multipole moments are calculated in section V using the graviton mode function determined in section IV. An analytic expression for the moments is given in terms of two integrals, which are then evaluated numerically. In appendix A we discuss the spheroidal wave functions. The differential equation of spheroidal wave functions is introduced and its solutions examined. We introduce a useful notation for the spheroidal wave functions, and give a practical method for evaluating them. Finally in appendix B we describe the numerical techniques used to evaluate the spheroidal wave functions and the two multipole moment integrals.

Throughout this paper we use units where the speed of light $c = 1$. We retain Newton's gravitational constant G and Planck's constant $\hbar$ explicitly.

II. THE ANGULAR CORRELATION FUNCTION

We consider only the anisotropy of the cosmic background radiation (CBR) arising via the Sachs-Wolfe effect [1] from tensor perturbations (gravitational waves). The anisotropy is characterized by the two-point angular correlation function $C(\gamma)$, where γ is the angle between two points located on the celestial sphere. The correlation function may be expanded in terms of Legendre Polynomials as

$$C(\gamma) = \left\langle \frac{\delta T}{T}(0) \frac{\delta T}{T}(\gamma) \right\rangle = \sum_{l=0}^{\infty} \frac{(2l+1)}{4\pi} \langle a_l^2 \rangle P_l(\cos\gamma). \tag{2.1}$$

The expansion coefficients $\langle a_l^2 \rangle$ are referred to as the multipole moments. The multipole moments are given in terms of an integral over graviton wavenumber k,

$$\langle a_l^2 \rangle \equiv 4\pi^2 (l+2)(l+1)l(l-1) \int_0^{\infty} \frac{dk}{k} |I_l(k)|^2, \tag{2.2}$$

where the function $I_l(k)$ is proportional to the Sachs-Wolfe integral along null geodesics, and is given by

$$I_l(k) \equiv \int_0^{\eta_0 - \eta_{\rm ls}} d\lambda \, F(\lambda, k) \frac{j_l(k(\eta_0 - \eta_{\rm ls} - \lambda))}{k(\eta_0 - \eta_{\rm ls} - \lambda)^2}. \tag{2.3}$$

Here $\eta_{\rm ls}$ is the time of last-scattering, and η_0 is the conformal time today. The function $j_l(z)$ is a spherical Bessel function of the first kind [15]. The function $F(\lambda, k)$ is proportional to the first derivative of the graviton mode function $\phi(\eta, k)$, and is defined by

$$F(\lambda, k) \equiv k^{1/2} \Big[\frac{\partial}{\partial \eta} \phi(\eta, k) \Big]_{\eta = \eta_{\rm ls} + \lambda}. \tag{2.4}$$

The graviton mode function obeys the massless Klein-Gordon or wave equation

$$\ddot{\phi} + 2\frac{\dot{a}(\eta)}{a(\eta)} \dot{\phi} + k^2 \phi = 0, \tag{2.5}$$

where $a(\eta)$ is the scale factor and

$$\cdot \equiv \frac{\partial}{\partial \eta}. \tag{2.6}$$

The mode function must satisfy the Wronskian normalization condition

$$\{ \phi(\eta, k) \dot{\phi}^*(\eta, k) - \phi^*(\eta, k) \dot{\phi}(\eta, k) \} = -\frac{2i\hbar G}{\pi^2 a^2(\eta)}. \tag{2.7}$$

The only physical input required is the choice of an initial quantum state for the gravitational field, which amounts to a choice of boundary conditions for the wave equation (2.5).

These formula for the angular correlation function are very general; a detailed and complete derivation is given in [2]. To calculate the correlation function (or equivalently the multipole moments) for any particular cosmological model, one need only to solve the wave equation (2.5) for the graviton mode function, and substitute into the formulae (2.1-2.4).

III. THE COSMOLOGICAL MODEL

The spacetime considered here is a spatially flat, perturbed FRW universe. The metric is

$$ds^2 = a^2(\eta)[-d\eta^2 + (\delta_{ij} + h_{ij}(\eta, x^k))dx^i dx^j], \tag{3.1}$$

where δ_{ij} is the flat metric of R^3, η is the conformal time, and $a(\eta)$ is the cosmological length scale or scale factor. The scale factor satisfies the Einstein equations

$$\frac{\dot{a}^2(\eta)}{a^4(\eta)} = \frac{8\pi G}{3}\rho(\eta) \text{ and } \frac{\ddot{a}(\eta)}{a^3(\eta)} - \frac{\dot{a}^2(\eta)}{a^4(\eta)} = -\frac{4\pi G}{3}\Big(\rho(\eta) + 3P(\eta)\Big), \tag{3.2}$$

where $\rho(\eta)$ is the energy density and $P(\eta)$ the pressure of the cosmological fluid. The metric perturbation h_{ij} is assumed to be small; in the limit as h_{ij} vanishes the spacetime is an unperturbed FRW universe. We have chosen a gauge so that the tensor perturbation h_{ij} has only spatial components.

In the absence of the metric perturbation h_{ij}, the background spacetime is a spatially flat FRW universe. Since the spacetime is spatially flat, the density parameter Ω_0, which is the ratio of the present-day energy density ρ_0 to the critical energy density required to produce a spatially flat universe, is equal to unity:

$$\Omega_0 = \frac{8\pi G\rho_0}{3H_0^2} = 1. \tag{3.3}$$

To specify the model, we need to give the scale factor $a(\eta)$. We do this in such a way that the model is completely defined by the minimal set of free parameters given in Table I. *All* our results, including the final expression (5.2), can be expressed in terms of this minimal set of parameters. For clarity, we often define auxiliary quantities and express results in terms of them; the auxiliary quantities can be expressed in terms of the parameters in Table I. In typical inflationary models, the free parameters in Table I have values of order H_0 between 50 and 100 km s^{-1} Mpc^{-1}, $100 < Z_{\rm ls} < 1500$, $2 \times 10^3 < Z_{\rm eq} < 2 \times 10^4$, and $10^{20} < Z_{\rm end}$. For a review of inflationary cosmology see reference [16].

A. The Inflationary or de Sitter Phase

Our cosmological model passes through two phases. The first phase is a de Sitter or inflationary phase. During the de Sitter phase the universe expands exponentially (expressed in terms of *comoving* time t, the scale factor behaves like $a(t) \sim e^{Ht}$, where H is the Hubble constant). In terms of conformal time, the scale factor is

$$a(\eta) = a(\eta_{\rm end})\Big(2 - \frac{\eta}{\eta_{\rm end}}\Big)^{-1} \text{ for } \eta \le \eta_{\rm end}, \tag{3.4}$$

where $\eta_{\rm end}$ is the conformal time at the end of the de Sitter phase. In terms of the parameters listed in Table I,

$$a(\eta_{\rm end}) = (1+Z_{\rm end})^{-1}, \tag{3.5}$$

$$\eta_{\rm end} = H_0^{-1}\left[\frac{(2+Z_{\rm eq})}{(2+Z_{\rm eq}+Z_{\rm end})(1+Z_{\rm end})}\right]^{1/2} \approx H_0^{-1}\frac{\sqrt{Z_{\rm eq}}}{Z_{\rm end}}, \tag{3.6}$$

where we have set the scale factor today $a(\eta_0) = 1$. During the de Sitter phase the energy density $\rho_{\rm dS}$ is constant and given by

$$\rho_{\rm dS} = \frac{3}{8\pi G}\frac{\dot{a}^2(\eta_{\rm end})}{a^4(\eta_{\rm end})} = \frac{3H_0^2}{8\pi G}\frac{(1+Z_{\rm end})^3}{(2+Z_{\rm eq})}(2+Z_{\rm eq}+Z_{\rm end}) \approx \frac{3}{8\pi G}H_0^2\frac{Z_{\rm end}^4}{Z_{\rm eq}} = \frac{Z_{\rm end}^4}{Z_{\rm eq}}\rho_0. \tag{3.7}$$

The pressure during the de Sitter phase is negative and constant, and is given by

$$P_{\rm dS} = -\rho_{\rm dS}. \tag{3.8}$$

The de Sitter phase is followed by a mixed phase.

B. The Mixed Radiation and Dust Phase

Immediately following the de Sitter phase is a mixed phase containing both dust and radiation. The scale factor is

$$a(\eta) = a(\eta_{\rm end})\left[\frac{1}{4}\left(\frac{\xi}{1+\xi}\right)\left(\frac{\eta}{\eta_{\rm end}}-1\right)^2 + \frac{\eta}{\eta_{\rm end}}\right] \text{ for } \eta \geq \eta_{\rm end}. \tag{3.9}$$

The constant ξ is defined in terms of the free parameters by

$$\xi = \frac{1+Z_{\rm eq}}{1+Z_{\rm end}}. \tag{3.10}$$

The stress-energy tensor is that of a perfect fluid with energy density

$$\rho(\eta) = \rho_{\rm dust}(\eta) + \rho_{\rm rad}(\eta) \text{ for } \eta \geq \eta_{\rm end}, \tag{3.11}$$

where the energy density for the dust $\rho_{\rm dust}(\eta)$, and for the radiation $\rho_{\rm rad}(\eta)$, are

$$\rho_{\rm dust}(\eta) = \frac{\rho_{\rm eq}}{2}\frac{a^3(\eta_{\rm eq})}{a^3(\eta)}, \tag{3.12}$$

$$\rho_{\rm rad}(\eta) = \frac{\rho_{\rm eq}}{2}\frac{a^4(\eta_{\rm eq})}{a^4(\eta)}. \tag{3.13}$$

Here $\rho_{\rm eq} = \rho(\eta_{\rm eq})$ is the energy density at conformal time $\eta_{\rm eq}$, when the dust and radiation energy densities are equal, and is given by

$$\rho_{\rm eq} = \frac{3H_0^2}{4\pi G}\frac{(1+Z_{\rm eq})^4}{(2+Z_{\rm eq})} \approx 2\left(\frac{Z_{\rm eq}}{Z_{\rm end}}\right)^4\rho_{\rm dS} \approx 2Z_{\rm eq}^3\rho_0. \tag{3.14}$$

The pressure of the cosmological fluid $P(\eta)$ is

$$P(\eta) = P_{\rm rad}(\eta) = P_{\rm eq}\frac{a^4(\eta_{\rm eq})}{a^4(\eta)} \text{ for } \eta \geq \eta_{\rm end}, \tag{3.15}$$

where the pressure at dust/radiation equality $P_{\rm eq}$ is

$$P_{\rm eq} = P(\eta_{\rm eq}) = \frac{\rho_{\rm eq}}{6}. \tag{3.16}$$

By inspection of (3.13),(3.15), and (3.16) one sees that

$$P(\eta) = P_{\rm rad}(\eta) = \frac{1}{3}\rho_{\rm rad}(\eta), \tag{3.17}$$

which is the relation between the pressure and energy density one would expect since the dust has zero pressure and the pressure is due entirely to the radiation present. The scale factor at $\eta_{\rm eq}$ is

$$a(\eta_{\rm eq}) = (1 + Z_{\rm eq})^{-1}. \tag{3.18}$$

One can express $\eta_{\rm eq}$ in terms of the conformal time at the end of the de Sitter phase $\eta_{\rm end}$ and the constant ξ as

$$\eta_{\rm eq} = \frac{\eta_{\rm end}}{\xi}(2\sqrt{2(1+\xi)} - 2 - \xi) \approx H_0^{-1}\frac{2(\sqrt{2}-1)}{\sqrt{Z_{\rm eq}}}. \tag{3.19}$$

For $\eta \ll \eta_{\rm eq}$ the energy density (3.11) varies as $\rho(\eta) \sim a^{-4}(\eta)$ and the cosmological model is radiation dominated, and for $\eta \gg \eta_{\rm eq}$ the energy density varies as $\rho(\eta) \sim a^{-3}(\eta)$ and the model is dust dominated. The model makes a smooth transition at $\eta = \eta_{\rm eq}$ from being radiation to dust dominated.

IV. THE GRAVITON MODE FUNCTION

To calculate the multipole moments for the cosmological model described above, one must first solve the wave equation (2.5) for the graviton mode function. We first solve for the "natural" positive- and negative-frequency mode functions during both the de Sitter and the mixed phases. We then make an appropriate choice of initial mode function during the de Sitter phase. This choice of initial mode function completely determines the graviton mode function for all later times. We express the mode function at later times using Bogolubov coefficient notation.

A. The de Sitter Phase

The solution to the wave equation (2.5) for the de Sitter phase can be expressed in terms of spherical Hankel functions. The scale factor during the de Sitter phase is given in (3.4). By making the change of dependent variable

$$\chi(\eta, k) = (\eta - 2\eta_{\rm end})^{-2}\phi(\eta, k), \tag{4.1}$$

and the change of independent variable

$$z = k(\eta - 2\eta_{\rm end}), \tag{4.2}$$

the wave equation can be expressed in the form

$$\frac{d^2\chi}{dz^2} + \frac{2}{z}\frac{d\chi}{dz} + \Big(1 - \frac{2}{z^2}\Big)\chi = 0. \tag{4.3}$$

This is Bessel's differential equation, and the solutions are spherical Bessel or Hankel functions [15]. Using the normalization condition (2.7) one obtains for the positive-frequency mode function during the de Sitter phase

$$\phi^{(+)}_{\rm ds}(\eta, k) = -i\sqrt{\frac{8}{3\pi}\frac{\rho_{\rm dS}}{\rho_P}}\, e^{-ik\eta_{\rm end}}\, \eta^2_{\rm end} k^{1/2} \frac{a^2(\eta_{\rm end})}{a^2(\eta)} h^{(2)}_1\Big(k(\eta - 2\eta_{\rm end})\Big), \tag{4.4}$$

where $h^{(2)}_1(z)$ is a spherical Hankel function of the second kind [15], and $\rho_P = 1/\hbar G^2 \approx 5 \times 10^{93}{\rm gm/cm}^3$ is the Planck energy density. The negative-frequency mode function during the de Sitter phase $\phi^{(-)}_{\rm ds}(\eta, k)$ is just the complex conjugate of the positive-frequency mode function (4.4). The positive- and negative-frequency mode functions form a complete solution to the wave equation for the de Sitter phase.

B. The Mixed Radiation and Matter Phase

The wave equation during the mixed radiation and dust phase ($\eta > \eta_{\rm end}$) can be cast in the form of the spheroidal wave function differential equation. By making the change of dependent variable

$$\chi(\eta, k) \equiv a^{1/2}(\eta)\phi(\eta, k), \tag{4.5}$$

the wave equation (2.5) becomes

$$\ddot{\chi} + \frac{\dot{a}(\eta)}{a(\eta)}\dot{\chi} + \Big(k^2 - \frac{1}{4}\frac{\dot{a}^2(\eta)}{a^2(\eta)} - \frac{1}{2}\frac{\ddot{a}(\eta)}{a(\eta)}\Big)\chi = 0. \tag{4.6}$$

One may define a new independent variable

$$x \equiv \sqrt{1 + \frac{a(\eta)}{a(\eta_{\rm eq})}}, \tag{4.7}$$

so that

$$\frac{dx}{d\eta} = \frac{1}{2x}\frac{\dot{a}(\eta)}{a(\eta_{\rm eq})}. \tag{4.8}$$

Using (4.7) and (4.8) one may write the wave equation (4.6) in the form

$$\frac{d^2\chi}{dx^2} + \Big[2x\frac{\ddot{a}(\eta)a(\eta_{\rm eq})}{\dot{a}^2(\eta)} - \frac{1}{x} + 2x\frac{a(\eta_{\rm eq})}{a(\eta)}\Big]\frac{d\chi}{dx}$$
$$+ \Big[4k^2x^2\frac{a^2(\eta_{\rm eq})}{\dot{a}^2(\eta)} - x^2\frac{a^2(\eta_{\rm eq})}{a^2(\eta)} - 2x^2\frac{\ddot{a}(\eta)a^2(\eta_{\rm eq})}{\dot{a}^2(\eta)a(\eta)}\Big]\chi = 0. \tag{4.9}$$

This expression can be simplified using the Einstein equations (3.2), along with (3.11) and (4.7) One can show that

$$\dot{a}^2(\eta) = 2x^2\ddot{a}(\eta)a(\eta_{\rm eq}), \tag{4.10}$$

and using this expression one may write the wave equation (4.9) as

$$\frac{d^2\chi}{dx^2} + 2x\frac{a(\eta_{\rm eq})}{a(\eta)}\frac{d\chi}{dx} + \Big[2k^2\frac{a(\eta_{\rm eq})}{\ddot{a}(\eta)} - x^2\frac{a^2(\eta_{\rm eq})}{a^2(\eta)} - \frac{a(\eta_{\rm eq})}{a(\eta)}\Big]\chi = 0. \tag{4.11}$$

Since from (4.7)

$$\frac{a(\eta_{\rm eq})}{a(\eta)} = \frac{1}{x^2-1}, \tag{4.12}$$

and from (3.9) and (3.10)

$$\frac{\ddot{a}(\eta)}{a(\eta_{\rm eq})} = \frac{1}{2\eta_{\rm end}^2}\Big(\frac{\xi^2}{1+\xi}\Big), \tag{4.13}$$

the wave equation becomes

$$\frac{d^2\chi}{dx^2} - \frac{2x}{(1-x^2)}\frac{d\chi}{dx} + \Big\{\frac{2}{(1-x^2)} + 4\kappa - \frac{1}{(1-x^2)^2}\Big\}\chi = 0. \tag{4.14}$$

Here κ is defined by

$$\kappa \equiv \Big(\frac{1+\xi}{\xi^2}\Big)k^2\eta_{\rm end}^2 = \frac{4\pi^2}{\lambda_0^2H_0^2}\frac{(2+Z_{\rm eq})}{(1+Z_{\rm eq})^2} \approx \frac{4\pi^2}{\lambda_0^2H_0^2Z_{\rm eq}}, \tag{4.15}$$

where λ_0 is the *present* day wavelength of the mode with wavenumber k. For the multipole moments of interest, $l \in [2, 1000]$, the contributions typically come from wavelengths in the range $\kappa \in [10^{-3}, 10^3]$. This form of the wave equation is the spheroidal wave function differential equation (A1), which is discussed in detail in appendix A.

The solutions to the wave equation (2.5) during the mixed phase can be expressed in terms of spheroidal wave functions. By inspection of (4.7) one sees that $x > 1$, and so the possible solutions to the wave equation (4.14) may be expressed as sums of any pair of

$$\chi(x,\kappa) = {}^j\mathsf{S}_2^1(x,\kappa), \;\; j = 1,2,3,4, \tag{4.16}$$

where ${}^j\mathsf{S}_2^1(x,\kappa)$ is a spheroidal wave function. Using (4.5), (4.16), the normalization condition (2.7), and the Wronskian relation (A22), one obtains a positive-frequency mode function during the mixed phase

$$\phi^{(+)}_{\rm mix}(\eta,k) = -2i\sqrt{\frac{8}{3\pi}\frac{\rho_{\rm dS}}{\rho_P}\frac{a(\eta_{\rm end})}{a(\eta)}\Bigl(\frac{1+\xi}{\xi}\Bigr)}\,\eta_{\rm end}^2 k^{1/2}\ {}^4\mathsf{S}^1_2(x,\kappa). \tag{4.17}$$

Note that x is a function of the conformal time η and κ depends on the wavenumber k. The negative-frequency mode function $\phi^{(-)}_{\rm mix}(\eta,k) = \Bigl[\phi^{(+)}_{\rm mix}(\eta,k)\Bigr]^*$ is just the complex conjugate of the positive-frequency mode function. The positive and negative frequency mode functions form a complete solution to the wave equation during the mixed radiation and matter phase. Note that the choice of graviton mode function during the de Sitter phase completely determines the mode function at all later times. Thus, the choice (4.17) of "positive-frequency" during the mixed phase is unimportant.

C. The Graviton Mode Function Expressed Using Bogolubov Coefficient Notation

The choice of mode function during the de Sitter phase completely determines the mode function at all later times. This is because a solution to the wave equation depends only on the values of ϕ and $\dot{\phi}$ on a spacelike Cauchy surface (ie. a surface of constant η). We choose the mode function during the de Sitter phase to be the pure positive-frequency de Sitter solution (4.4). This is the unique solution corresponding to a de Sitter-invariant vacuum state with the same (Hadamard) short distance behavior as one would find in Minkowski space [17]. Having made this choice for the mode function during the de Sitter phase, the mode function during all times is

$$\phi(\eta,k) = \begin{cases} \phi^{(+)}_{\rm ds}(\eta,k) & \eta \le \eta_{\rm end},\ \text{de Sitter phase}, \\ \\ \alpha(k\eta_{\rm end})\phi^{(+)}_{\rm mix}(\eta,k) + \beta(k\eta_{\rm end})\phi^{(-)}_{\rm mix}(\eta,k) & \eta \ge \eta_{\rm end},\ \text{mixed phase}, \end{cases} \tag{4.18}$$

where α and β are Bogolubov coefficients.

The Bogolubov coefficients are determined by requiring that the mode function and its first derivative be continuous at $\eta = \eta_{\rm end}$. One obtains

$$\begin{aligned} \alpha(k\eta_{\rm end}) &= k\eta_{\rm end}\sqrt{\frac{1+\xi}{\xi}}\Biggl\{\Bigl[\frac{\xi}{\sqrt{1+\xi}}\,{}^3\mathsf{S}^{1\prime}_2(x_1,\kappa) - {}^3\mathsf{S}^1_2(x_1,\kappa)\Bigr]\frac{i}{2k\eta_{\rm end}}\Bigl(1+\frac{i}{k\eta_{\rm end}}\Bigr) - {}^3\mathsf{S}^1_2(x_1,\kappa)\Biggr\}, \\ \beta(k\eta_{\rm end}) &= k\eta_{\rm end}\sqrt{\frac{1+\xi}{\xi}}\Biggl\{\Bigl[\frac{\xi}{\sqrt{1+\xi}}\,{}^4\mathsf{S}^{1\prime}_2(x_1,\kappa) - {}^4\mathsf{S}^1_2(x_1,\kappa)\Bigr]\frac{i}{2k\eta_{\rm end}}\Bigl(1+\frac{i}{k\eta_{\rm end}}\Bigr) - {}^4\mathsf{S}^1_2(x_1,\kappa)\Biggr\}. \end{aligned} \tag{4.19}$$

The prime in (4.19) is defined by

$${}^j\mathsf{S}^{\mu\prime}_\lambda(x_1,\theta) \equiv \Bigl[\frac{\partial}{\partial z}\,{}^j\mathsf{S}^\mu_\lambda(z,\theta)\Bigr]_{z=x_1}, \tag{4.20}$$

where

$$x_1 \equiv \sqrt{1+\frac{a(\eta_{\rm end})}{a(\eta_{\rm eq})}} = \sqrt{1+\xi}. \tag{4.21}$$

Using the Wronskian relation for the spheroidal wave functions (A22) one can easily verify that

$$|\alpha(k\eta_{\rm end})|^2 - |\beta(k\eta_{\rm end})|^2 = 1. \tag{4.22}$$

We stress again that *the choice of graviton mode function during the de Sitter phase completely determines the mode function at all later times*. Thus, the choice of "positive-frequency" during the mixed phase is unimportant. Had we chosen a different solution to the wave equation during the mixed phase to call "positive-frequency", then the Bogolubov coefficients (4.19) would be different in such a way so that the mode function (4.18) *would be the same*.

V. MULTIPOLE MOMENTS

Having determined the graviton mode function for our cosmological model, we may calculate the angular correlation function $C(\gamma)$, or equivalently, the multipole moments $\langle a_l^2 \rangle$. We simply substitute the graviton mode function (4.18) into the formulae (2.1-2.4).

A. Analytical Results

The graviton mode function (4.18) is exact; no approximations (ie. long wavelength) have been made. One may directly substitute the mode function into the formulae (2.1-2.4) to obtain an exact expression for the multipole moments; because the arguments of the spheroidal wave functions in (4.18) are functions themselves, however, the result is complicated and not very illuminating. In typical inflationary models, the amount of expansion is very large. If one takes the limit $Z_{\rm end} \to \infty$, then $\xi \to 0$. This allows one to write a fairly compact expression for the multipole moments; after substituting the mode function (4.18) into the formulae (2.1-2.4), one may collect together terms in the expression for the multipole moments $\langle a_l^2 \rangle$ which are the same order in ξ. Then in the limit as $Z_{\rm end} \to \infty$ and $\xi \to 0$, one may consider only the leading term. The leading term, which is $\mathrm{O}(\xi^0)$, is given below in (5.2). The neglected terms are $\mathrm{O}(\xi^1)$ or greater. For typical inflationary models one has $Z_{\rm end} \gtrsim 10^{20}$ and $Z_{\rm eq} \approx 10^4$, so that $\xi \lesssim 10^{-16}$. So the expression (5.2) is quite accurate for most cosmological models, since the neglected terms are very small.

The expressions for the multipole moments $\langle a_l^2 \rangle$ are fairly simple. After substituting the mode function (4.18) into the formulae (2.1-2.4), and making the same changes of variable as in section IV B, ie.

$$x \equiv \sqrt{1 + \frac{a(\eta)}{a(\eta_{\rm eq})}} \quad \text{and} \quad \kappa \equiv \left(\frac{1+\xi}{\xi^2}\right) k^2 \eta_{\rm end}^2, \tag{5.1}$$

one obtains for the multipole moments ($l \geq 2$)

$$\langle a_l^2 \rangle = \frac{4}{3}\pi^2 \frac{(l+2)!}{(l-2)!} \frac{\rho_{\rm dS}}{\rho_P} \int_0^\infty \frac{d\kappa}{\kappa^{5/2}} \left\{ {}^1\mathsf{T}_2^1(x_1,\kappa) G_l^2(\kappa) - {}^2\mathsf{T}_2^1(x_1,\kappa) G_l^1(\kappa) \right\}^2 + \mathrm{O}(\xi^1). \tag{5.2}$$

The integral above is simply an integral over the (rescaled, dimensionless) wavenumber κ. The functions ${}^{j}\mathsf{T}^{1}_{2}(x_1,\kappa)$ are the same functions defined in (A20). The functions $G^{j}_{l}(\kappa)$ are the (reparametrized) Sachs-Wolfe integrals over null geodesics, given by

$$G^{j}_{l}(\kappa) \equiv \int_{x_{\rm ls}}^{x_o} dx \frac{J_{l+1/2}\Big(2\kappa^{1/2}(x_o-x)\Big)}{(x_o-x)^{5/2}(x^2-1)^{1/2}}\Big\{\frac{x}{x^2-1}{}^{j}\mathsf{S}^{1}_{2}(x,\kappa) - {}^{j}\mathsf{S}^{1\prime}_{2}(x,\kappa)\Big\}, \tag{5.3}$$

where the limits $x_{\rm ls}$ and x_o on the integral are given in terms of redshift by

$$x_o \equiv \sqrt{2+Z_{\rm eq}} \text{ and } x_{\rm ls} \equiv \sqrt{1+\frac{1+Z_{\rm eq}}{1+Z_{\rm ls}}}. \tag{5.4}$$

These formulae, and especially the spheroidal wave functions, may be numerically evaluated using the techniques discussed in appendix B. Henceforth we refer to (5.2) and (5.3) as the "mixed" formulae for the multipole moments. Furthermore, we refer to multipole moments calculated using (5.2) and (5.3) as the "mixed" multipoles.

B. Numerical Results

We have numerically evaluated the "mixed" formulae (5.2) and (5.3). The second column of Table II shows the "mixed" multipoles. The third column of Table II shows the results obtained by evaluating Eq. (6.2) of Allen and Koranda [2], which we refer to as the "exact-dust" formula for the multipole moments. The "exact-dust" formula assumes (1) the universe begins with an initial de Sitter phase, followed by (2) a pure radiation phase containing only radiation and no dust, followed by (3) a pure dust phase containing only dust and no radiation, during which (4) last-scattering takes place. We refer to this type of universe as a "dust" universe, to distinguish it from the model described by (3.9), (3.11), and (3.15), which we refer to as "mixed" universe because it contains both dust and radiation at last-scattering. The fourth column shows the results obtained by evaluating Eq. (6.1) of Allen and Koranda, which we refer to as the "approximate-dust" formula for the multipole moments. The "approximate-dust" formula is a long-wavelength approximation to the "exact-dust" formula, and is *equivalent* to the standard formulae for the multipole moments given by Abbott and Wise [5] and Starobinsky [6]. The fifth column shows recent results of Ng and Speliotopoulos [10], who numerically integrated the wave equation to obtain the amplitude of the gravitational wave (or graviton mode function). They also considered a universe model which contains both radiation and dust at last-scattering. All of the results in Table II were obtained with $Z_{\rm eq} = 6000$ and $Z_{\rm ls} = 1100$.

Figures 1,2, and 3 compare the "mixed" multipole moments to the multipole moments calculated using other techniques. The quantity M_l in Figures 1-3 is defined by

$$M_l \equiv \frac{l(l+1)}{6}\frac{\langle a_l^2\rangle}{\langle a_2^2\rangle}. \tag{5.5}$$

(Note that in [2] the equation defining M_l contains an extraneous factor of $\rho_{\rm ds}/\rho_{\rm P}$.) The points labeled "mixed" in Figure 1 show results obtained by numerically evaluating the "mixed" formulae (5.2) and (5.3). The points in Figure 1 labeled "transfer function" show

results from Turner, White, and Lidsey [9], who numerically integrate the wave equation, and express the solutions in terms of the standard long-wavelength approximate mode functions [2] using a "transfer function". The points in Figure 2 labeled "mixed" again show results obtained by numerically evaluating the "mixed" formulae. The points labeled "exact-dust" show results obtained using the "exact-dust" formula, and the points labeled "approximate-dust" show results obtained using the "approximate-dust" formula. Figure 3 compares the "mixed" results to results from Dodelson, Knox, and Kolb [12] (labeled "Boltzmann"), who do not use the Sachs-Wolfe formula to calculate the CBR anisotropy. Instead they use numerical methods to evolve the photon distribution function using first-order perturbation theory of the general relativistic Boltzmann equation for radiative transfer. All the multipole moments shown in Figures 1, 2, and 3 are for cosmological parameters $Z_{\rm eq} \approx 6000$ and $Z_{\rm ls} = 1100$. (The values of $Z_{\rm eq}$ for the Turner, White, and Lidsey work and for the the Dodelson, Knox, and Kolb results differs from 6000 by about one percent).

C. Discussion

The Ng and Speliotopoulos multipoles agree quite well with the "mixed" multipoles obtained here, using spheriodal wavefunctions, for a cosmology containing dust and radiation components. This is expected because the two methods used to calculate the multipole moments should be essentially equivalent. The graviton mode functions Ng and Speliotopoulos obtain by numerically integrating the wave equation (with the correct boundary conditions) must be equivalent to our analytic expressions (4.18). The cosmological model Ng and Speliotopoulos consider, however, is slightly different than our own. They model the smooth transition during the mixed phase by a simpler scale factor than our own (3.9). This may account for the small discrepancy between their results and our own.

The Dodelson, Knox, and Kolb (Figure 3) multipoles also appear consistent with the "mixed" multipoles. This is also expected since the Boltzmann formalism [11,12] and the Sachs-Wolfe formalism should yield equivalent results. We do not understand at this time the small discrepancy between the two multipole spectrums.

For $l \lesssim 30$, the "exact-dust" multipoles and the "approximate-dust" multipoles agree fairly well with the "mixed" multipoles (Figure 2). This is not surprising. The small l multipoles $\langle a_l^2 \rangle$ are most affected by longer wavelength perturbations. These longer wavelength perturbations were redshifted outside the Hubble sphere early in the inflationary phase, and only recently re-entered the Hubble sphere (the longest wavelength perturbations remain outside the Hubble sphere even today [16]). Because they remained outside the Hubble sphere until recently, the longer wavelength perturbations are insensitive to the details of the evolution of the universe before it became dust dominated. Thus, the "mixed" universe and "dust" universe models are essentially equivalent for longer wavelength perturbations. So it's not surprising that the same CBR anisotropies are produced by the long wavelength perturbations in either model. Thus the "exact-dust", "approximate-dust", and "mixed" multipoles should, and do, agree for small l. Furthermore, because the "approximate-dust" formula for the multipole moments is equivalent to the standard formulae given by Abbott and Wise [5] and Starobinsky [6], one can conclude that the standard formulae for the multipole moments are accurate for small l, whether or not the universe was completely dust dominated at last-scattering.

For $l \gtrsim 30$, the "exact-dust" multipoles and the "approximate-dust" multipoles differ significantly from the "mixed" multipoles. Again this is not surprising. The larger l multipoles are more affected by shorter wavelength perturbations, which re-entered the Hubble sphere before the universe became dust dominated, and are therefore sensitive to the details of the cosmological expansion before dust domination. A "mixed" universe becomes dust dominated *much more slowly* than a "dust" universe, which is dust dominated immediately after the radiation phase ends at dust/radiation equality $\eta_{\rm eq}$. Therefore the shorter wavelength modes in a "mixed" universe and a "dust" universe evolve very differently after they re-enter the Hubble sphere. This difference is evident in Figure 2 for the large l multipole moments.

The Turner, White, and Lidsey (TWL) multipole spectrum differs significantly from the "mixed" multipole spectrum (Figure 1). In particular their multipole moments are significantly greater than the "mixed" multipoles for $3 \lesssim l \lesssim 80$. Although TWL consider a "mixed" universe, they use the standard multipole moment formulae for a "dust" universe. However, they modify the standard formulae by including a time-independent transfer function $T(k/k_{\rm eq})$, which depends only on the wavenumber k. TWL give an explicit functional form for the transfer function, which they obtain by numerically integrating the wave equation [9]:

$$T(y) = [1.0 + 1.34y + 2.50y^2]^{1/2}, \text{ where } y = k/k_{\rm eq}. \tag{5.6}$$

Since the transfer function $T \geq 1$ appears in the expression for the multipole moments as $|T(k/k_{\rm eq})|^2$ (see Eqs. (22) and (23) of [9]), one can see that the effect of the transfer function (5.6) is to *increase* the multipole moments. Furthermore, the contribution from shorter wavelength (larger k) modes is enhanced more than the contribution from larger wavelength (smaller k) modes, since $T(k/k_{\rm eq}) \to 1$ as $k \to 0$.

Since the TWL multipoles are significantly greater than the "mixed" multipoles for $3 \lesssim l \lesssim 80$, *the transfer function overestimates the contribution to the multipole moments from longer wavelength modes.* This is easy to see. As discussed above, the standard formulae are accurate for small l multipoles, and give essentially the same results as the "mixed" formulae for $l \lesssim 30$. The TWL formulae for the multipole moments are equivalent to the standard formulae, except for the transfer function. Thus if the transfer function was set to unity, the TWL multipoles would be the same as the standard multipoles, and hence would be equivalent to the "mixed" multipoles for $l \lesssim 30$. Since the TWL multipoles are larger than the "mixed" multipoles for $3 \lesssim l \lesssim 80$, the transfer function must enhance the the contribution to the $3 \lesssim l \lesssim 80$ multipole moments too much. Because the small l moments are affected most by longer wavelength perturbations, the transfer function must overestimate the contribution from longer wavelengths, or smaller wavenumber k.

The TWL multipole spectrum is also significantly different than the "mixed" multipole spectrum for large l. The large l multipoles are most affected by shorter wavelength modes. The transfer function (5.6) significantly enhances the contribution of shorter wavelength modes (larger k) to the multipole moments. Because the TWL transfer function is time-independent, however, it can not alter the time evolution of the shorter wavelength modes. By comparing the "dust" universe graviton mode function (see Eq. (4.28) of [2])

$$\phi(\eta, k)_{\rm dust} = \sqrt{\frac{24}{\pi}\frac{\rho_{\rm dS}}{\rho_{\rm P}}}\frac{j_1\Big(k(\eta+\eta_{\rm eq})\Big)}{k^{5/2}(\eta+\eta_{\rm eq})}, \tag{5.7}$$

(which is equivalent to the standard formulae for the gravity-wave amplitude [2], and hence equivalent to the TWL formulae for the gravity-wave amplitude) to the "mixed" universe mode function (4.18), one can see that the time evolution of the shorter wavelength modes is very different in a "dust" universe when compared to the time evolution in a "mixed" universe. Thus one expects that for shorter wavelength modes, the integral along the null geodesics (2.3) in the Sachs-Wolfe formula will be very different for a "dust" universe, when compared to a "mixed" universe. Since the transfer function is time-independent, it has no effect on the integral (2.3). So one expects that the multipole spectrum for a "dust" universe will be very different than the multipole spectrum for a "mixed" universe, even with the transfer function included. Figure 1 shows that this is the case. In particular, the "bump" in the TWL multipole spectrum appears near $l \approx 180$, rather than $l \approx 200$, as for the "mixed" multipole spectrum.

VI. CONCLUSION

This paper examines the tensor perturbations of the gravitational field in a spatially flat, FRW cosmology containing a mixture of radiation and dust, and shows that they may be expressed in terms of spheroidal wave functions. Although spheroidal wave functions have appeared in this context before, previous authors incorrectly determined the characteristic exponent which labels these functions. After explaining the correct method for determining the characteristic exponent, we show that spheroidal wave functions may be efficiently and accurately evaluated using standard numerical techniques.

We considered inflationary cosmological models, and used the spheroidal wave functions to find the spectrum of CBR temperature fluctuations resulting from primordial tensor (gravitational radiation) perturbations. These temperature fluctuations are predicted by all inflationary models. Their existence follows from first principles: it is a consequence of the uncertainty principle and the Einstein equation. The temperature fluctuations have been previously studied by a number of authors (including ourselves) using a variety of approximations, and both analytic and numerical techniques.

In hindsight, only two approximations remain in this work. One is that the amplitude of the gravitational perturbation h_{ij} is very small. This approximation is indeed well justified. The second approximation is that the energy density and pressure of the universe correspond to a mixture of dust and radiation as given in (3.11-3.15). Going back in time, this approximation is good until approximately the time of nucleosynthesis, $t = 200$ seconds, when the number of effectively massless particles in the universe changed. This should not affect the multipole moments $\langle a_l^2 \rangle$ which we consider, which have $l < 300$. For larger values of l, other physical effects such as the finite thickness of the surface of last scattering may also become relevant.

It is likely that the spheroidal wave functions, which describe gravitational wave perturbations in realistic cosmological models, will find other useful applications. We expect that the results and methods of this paper may prove applicable to a wider variety of calculations than the CBR temperatures perturbations considered here.

ACKNOWLEDGMENTS

We are grateful to Scott Dodelson, Edward Kolb, Lloyd Knox, Jorma Louko, and Mike Turner for useful comments and suggestions. This work has been partially supported by NSF Grant No. PHY91-05935.

APPENDIX A

In spatially flat FRW universes, graviton mode functions in a linearized theory of gravity obey a minimally-coupled, massless, scalar wave equation [18] like (2.5). If the scale factor of the spatially flat FRW universe transforms smoothly from being radiation to dust dominated, the solutions to the equation are spheroidal wave functions.

1. The Differential Equation of Spheroidal Wave Functions and Its Solutions

There is no generally accepted form for the differential equation of spheroidal wave functions. We write the differential equation as

$$\frac{d^2\varphi}{dz^2} - \frac{2z}{(1-z^2)}\frac{d\varphi}{dz} + \left\{\frac{\lambda}{(1-z^2)} + 4\theta - \frac{\mu^2}{(1-z^2)^2}\right\}\varphi = 0. \tag{A1}$$

The parameters μ, λ, and θ and the variable z can in general be complex. Here we take z,λ, μ, and θ to be real. We also consider only $\theta \geq 0$. The differential equation (A1) has two regular singular points at $z = \pm 1$ and an irregular singular point at $z = \infty$. We only consider $z > 1$. Then the solutions of (A1) are the *spheroidal wave functions* [19,20]

$$\varphi = S_\nu^{\mu(j)}(z, \theta), \;\; z > 1, \;\; j = 1, 2, 3, 4. \tag{A2}$$

The parameter μ is the *order* of the spheroidal wave function, and ν is the *characteristic exponent*. In later sections we consider in detail the characteristic exponent ν and its relation to the order μ and the parameters λ and θ. For now we simply note that ν is restricted so that

$$\nu + 1/2 \neq \text{ integer}. \tag{A3}$$

For a very thorough and complete discussion of the differential equation (A1) and the solutions (A2) see reference [20].

The spheroidal wave functions can be expressed in terms of more familiar special functions. If $\theta = 0$ then the differential equation (A1) reduces to Legendre's differential equation, suggesting that the spheroidal wave functions can be expressed in terms of Legendre functions [19,20]. For $z > 1$, however, it is more useful to express the spheroidal wave functions as infinite sums of Bessel functions. For $\mu > 0$ one can write the spheroidal functions as

$$S_\nu^{\mu(j)}(z, \theta) = \left(\frac{z^2}{z^2 - 1}\right)^{\mu/2} T_\nu^{\mu(j)}(z, \theta), \;\; \mu > 0, \tag{A4}$$

where $T_\nu^{\mu(j)}(z, \theta)$ is the infinite sum

$$T_\nu^{\mu(j)}(z,\theta) = s_\nu^\mu(\theta) \sum_{r=-\infty}^{\infty} a_{\nu,r}^\mu(\theta) \psi_{\nu+2r}^{(j)}(2\theta^{1/2} z), \;\; j = 1,2,3,4. \tag{A5}$$

The expansion coefficients $a_{\nu,r}^\mu(\theta)$ and the normalization factor $s_\nu^\mu(\theta)$, which are the same for any j, are discussed below. The functions $\psi_\upsilon^{(j)}(z)$ are proportional to Bessel or Hankel functions:

$$\begin{aligned}
\psi_\upsilon^{(1)}(z) &= \sqrt{\tfrac{\pi}{2z}} J_{\upsilon+1/2}(z), \\
\psi_\upsilon^{(2)}(z) &= \sqrt{\tfrac{\pi}{2z}} Y_{\upsilon+1/2}(z), \\
\psi_\upsilon^{(3)}(z) &= \sqrt{\tfrac{\pi}{2z}} H_{\upsilon+1/2}^{(1)}(z), \\
\psi_\upsilon^{(4)}(z) &= \sqrt{\tfrac{\pi}{2z}} H_{\upsilon+1/2}^{(2)}(z).
\end{aligned} \tag{A6}$$

The spheroidal wave function of the first kind ($j = 1$) and the spheroidal wave function of the second kind ($j = 2$) form a complete solution to the differential equation (A1). Because the Hankel functions $H_\upsilon^{(1)}(z) = J_\upsilon(z) \pm i Y_\upsilon(z)$ can be written as linear combinations of Bessel functions (see equation (3.86) in reference [15]), the spheroidal functions of the third ($j = 3$) and fourth ($j = 4$) kind can be written as linear combinations of spheroidal functions of the first and second kind:

$$\begin{aligned}
S_\nu^{\mu(3)}(z,\theta) &= S_\nu^{\mu(1)}(z,\theta) + i S_\nu^{\mu(2)}(z,\theta), \\
S_\nu^{\mu(4)}(z,\theta) &= S_\nu^{\mu(1)}(z,\theta) - i S_\nu^{\mu(2)}(z,\theta).
\end{aligned} \tag{A7}$$

The spheroidal functions of the third and fourth kind also form a complete solution to the spheroidal differential equation. The expansions (A4) of the spheroidal wave functions in terms of Bessel and Hankel functions are only useful if the infinite sums (A5) converge.

The convergence of the infinite sums depends on the expansion coefficients $a_{\nu,r}^\mu(\theta)$. Substituting (A4) and (A5) into the differential equation (A1) yields a three-term recurrence relation that the expansion coefficients must satisfy. The recurrence relation can be written as

$$\mathcal{A}_{\nu,r}^\mu(\theta) a_{\nu,r-1}^\mu(\theta) + \mathcal{B}_{\nu,r}^\mu(\theta) a_{\nu,r}^\mu(\theta) + \mathcal{C}_{\nu,r}^\mu(\theta) a_{\nu,r+1}^\mu(\theta) = 0, \tag{A8}$$

where

$$\begin{aligned}
\mathcal{A}_{\nu,r}^\mu(\theta) &= 4\theta \frac{(\nu+2r-\mu)(\nu+2r-\mu-1)}{(2\nu+4r-3)(2\nu+4r-1)}, \\
\mathcal{B}_{\nu,r}^\mu(\theta) &= \lambda - (\nu+2r)(\nu+2r+1) + \frac{(\nu+2r)(\nu+2r+1)+\mu^2-1}{(2\nu+4r-1)(2\nu+4r+3)} 8\theta, \\
\mathcal{C}_{\nu,r}^\mu(\theta) &= 4\theta \frac{(\nu+2r+\mu+2)(\nu+2r+\mu+1)}{(2\nu+4r+3)(2\nu+4r+5)}.
\end{aligned} \tag{A9}$$

The solution to this recurrence relation, as well as the convergence of the infinite sums (A5), depends critically on the parameters μ, ν, λ, and θ, and is discussed below. Once a solution to the recurrence relation (for which the infinite sums (A5) converge) is obtained, the normalization factor $s_\nu^\mu(\theta)$ is given by

$$s_\nu^\mu(\theta) = [\sum_{r=-\infty}^{\infty} (-1)^r a_{\nu,r}^\mu(\theta)]^{-1}. \tag{A10}$$

This normalization is chosen so that in the limit as z becomes very large

$$\lim_{z\to\infty} \left[S_\nu^{\mu(j)}(z,\theta)/\psi_\nu^{(j)}(2\theta^{1/2}z)\right] = 1. \tag{A11}$$

This relation and many more details of the solutions (A4) are developed in reference [20].

2. The Eigenvalue λ

Although the order μ of the spheroidal wave function, along with the parameters θ and λ, appears directly in the differential equation (A1), the characteristic exponent ν does not. In most investigations and applications of spheroidal wave functions [19,20,21,22], however, the parameter λ is left unfixed; one *assumes* a (typically integer) value for ν and considers λ to be a function of μ, ν, and θ and writes

$$\lambda = \lambda_\nu^\mu(\theta). \tag{A12}$$

$\lambda_\nu^\mu(\theta)$ is often referred to as an eigenvalue, especially when considering spheroidal wave functions as solutions to the three-dimensional wave equation [23].

For a given choice of the parameters μ, ν, and θ, the eigenvalue $\lambda_\nu^\mu(\theta)$ is that value of λ for which the recurrence relation (A8) has a *minimal* solution. A minimal solution, roughly speaking, is a set of coefficients $a_{\nu,r}^\mu(\theta)$ that satisfy the recurrence relation *and* fall off for large $|r|$ [24]. A *dominant* solution is a set of coefficients that satisfy the recurrence relation but do not fall off. If the solution to the recurrence relation is a dominant solution, the coefficients $a_{\nu,r}^\mu(\theta)$ do not fall off for large $|r|$, and the infinite sums in (A5) may not converge. In general a three-term recurrence relation will have two independent solutions, much like a second-order, ordinary differential equation. However, neither of the two solutions, nor any linear combination of the two solutions, need be a minimal solution [24]. For a given set of parameters μ, ν, and θ, a minimal solution to the recurrence relation (A8) exists only for a single, discrete value of λ. That value for which the minimal solution exists is the eigenvalue $\lambda_\nu^\mu(\theta)$. In our problem, we are given λ, θ, and μ. One can find ν (modulo an integer) by requiring that the recurrence relation (A8) have a minimal solution.

The functional relationship between the parameters μ, ν, θ and the eigenvalue $\lambda_\nu^\mu(\theta)$ is complicated. It has been shown [19] that the functional relationship can be expressed as

$$\cos(2\pi\nu) = f(\lambda, \mu^2, \theta), \tag{A13}$$

where a closed, analytic form for the function f is usually unattainable. The relation (A13) only determines the characteristic exponent ν (as a function of λ, μ, and θ) up to an integer; a second constraint [20] fixes ν:

$$\lambda_\nu^\mu(\theta = 0) = \nu(\nu + 1). \tag{A14}$$

In section IV B the special case of the differential equation (A1) with $\lambda = 2$ is considered. The constraint (A14), along with the condition (A3) that ν not be a half-integer, fixes ν so that

$$\frac{1}{2} < \nu < \frac{3}{2} \text{ for } \lambda = 2. \tag{A15}$$

For investigations of some of the analytic properties of $f(\lambda, \mu^2, \theta)$ see reference [20]. A more practical method for finding the functional relation between the parameters μ, ν, θ, and λ is discussed in section A 6.

3. The Case $\mu = 1$, $\lambda = 2$

The special case of the differential equation (A1) with $\mu = 1$ and $\lambda = 2$ is of cosmological interest, and has been previously studied by Sahni [13] and Nariai [14], who incorrectly take the solution to be $S_1^{1(4)}$. In spatially flat FRW universes containing a mixture of dust and radiation, one may cast the wave equation for graviton mode functions in the form of the spheroidal wave function differential equation, as shown in section IV B. The differential equation the graviton mode function obeys (4.14) is the special case of the differential equation (A1) with $\mu = 1$, $\lambda = 2$, and θ arbitrary. (θ is arbitrary since in section IV B it is proportional to the wave number of a graviton mode function, and we desire expressions for the mode functions that are valid for an interesting range of wavenumbers.) Even if one takes λ in (A1) to be fixed and does not consider the eigenvalue problem for λ, the arguments and conclusion in the previous paragraph are still valid, especially the constraint (A13); if μ, ν, λ, and θ do not satisfy (A13) a minimal solution to the recurrence relation does not exist and the infinite sums in (A5) do not converge. If $\lambda = 2$, $\mu = 1$, and θ is arbitrary, then the characteristic exponent ν is determined by the constraint (A13) with $\lambda = 2$ and $\mu = 1$. Tables of eigenvalues $\lambda_\nu^\mu(\theta)$ for different values of μ, ν, and θ have been published [22], however, and from these one can determine that the solution to (A13) for $\mu = 1$, $\lambda = 2$, and θ arbitrary is *not* $\nu = 1$, ie.

$$\cos(2\pi) \neq f(2, 1, \theta) \text{ for arbitrary } \theta. \tag{A16}$$

So for arbitrary θ the solution to the differential equation (A1) with $\mu = 1$ and $\lambda = 2$ is *not* the spheroidal wave function (A2) with $\mu = 1$ and $\nu = 1$, ie.

$$\varphi \neq S_1^{1(j)}(z, \theta) \text{ for } \lambda = 2. \tag{A17}$$

This subtle point is missed in [13,14], where the solution to the spheroidal wave function differential equation with $\mu = 1$, $\lambda = 2$, and θ arbitrary is incorrectly given as $S_1^{1(4)}$.

4. A More Suitable Notation

The notation introduced above for the spheroidal wave functions (A2) is most useful when the order μ and the characteristic exponent ν are fixed, and the eigenvalue $\lambda_\nu^\mu(\theta)$ is considered as a function of μ, ν, and θ. Since we are most interested in the case when μ and λ are fixed, it is more descriptive to denote the characteristic exponent as $\nu = \nu_\lambda^\mu(\theta)$. This convention, however, would have one denote the spheroidal wave functions as $S_{\nu_\lambda^\mu(\theta)}^{\mu(j)}(z, \theta)$, which is cluttered and inconvenient. In section IV B, where θ is itself a function (of wavenumber), the notation would be even more unpleasant.

For this reason we adopt a new notation for the spheroidal wave functions. The solution to the differential equation (A1) with μ and λ fixed is denoted

$$ {}^{j}\mathsf{S}^{\mu}_{\lambda}(z,\theta) \equiv S^{\mu(j)}_{\nu^{\mu}_{\lambda}(\theta)}(z,\theta). \tag{A18} $$

The function on the left-hand side above is, of course, the same function as on the right-hand side, expressed using a different notation. The indices μ and λ are those that appear in the differential equation, and again $j = 1, 2, 3, 4$. In terms of Bessel functions, the spheroidal wave function is now written as

$$ {}^{j}\mathsf{S}^{\mu}_{\lambda}(z,\theta) = \left(\frac{z^2}{z^2-1}\right)^{\mu/2} {}^{j}\mathsf{T}^{\mu}_{\lambda}(z,\theta), \tag{A19} $$

where

$$ {}^{j}\mathsf{T}^{\mu}_{\lambda}(z,\theta) \equiv s^{\mu}_{\lambda}(\theta) \sum_{r=-\infty}^{\infty} a^{\mu}_{\lambda,r}(\theta)\psi^{(j)}_{\nu+2r}(2\theta^{1/2}z), \tag{A20} $$

with $\nu = \nu^{\mu}_{\lambda}(\theta)$, and the $\psi^{(j)}_{v}$ are the same functions given in (A6). The expansion coefficients $a^{\mu}_{\lambda}(\theta)$ are the same as those in (A5) and obey the same recurrence relation (A8) with the obvious change in notation. The normalization factor $s^{\mu}_{\lambda}(\theta)$ is also the same as in (A5) with the obvious change in notation. We use this notation in sections IV B-V A, and the rest of this appendix.

5. Wronskian and Complex Conjugates

Two relations for the spheroidal wave functions are especially useful in section IV B. The first involves the spheroidal wave functions of the third and fourth kind, and is obvious from the relations (A7):

$$ {}^{4}\mathsf{S}^{\mu}_{\lambda}(z,\theta) = [{}^{3}\mathsf{S}^{\mu}_{\lambda}(z,\theta)]^{*}. \tag{A21} $$

Here a $*$ denotes complex conjugation. The second relation is the Wronskian for the spheroidal wave functions of the third and fourth kind:

$$ W[{}^{4}\mathsf{S}^{\mu}_{\lambda}(z,\theta), {}^{3}\mathsf{S}^{\mu}_{\lambda}(z,\theta)] \equiv {}^{4}\mathsf{S}^{\mu}_{\lambda}(z,\theta)\frac{d}{dz}{}^{3}\mathsf{S}^{\mu}_{\lambda}(z,\theta) - {}^{3}\mathsf{S}^{\mu}_{\lambda}(z,\theta)\frac{d}{dz}{}^{4}\mathsf{S}^{\mu}_{\lambda}(z,\theta) = \frac{i}{\theta^{1/2}(z^2-1)}. \tag{A22} $$

This relation, along with related results, is derived in reference [20] (see especially section 3.65, equation (53)).

6. A Practical Method for Determining $\nu^{\mu}_{\lambda}(\theta)$ and ${}^{j}\mathsf{S}^{\mu}_{\lambda}(z,\theta)$

The constraints (A13) and (A14) determine $\nu^{\mu}_{\lambda}(\theta)$ for a given choice of μ, λ, and θ. In practice, however, it is difficult to use these constraints since a closed, analytic form for the the function f is usually not known. Recall, though, that the constraint (A13) is equivalent

to finding a minimal solution to the recurrence relation (A8). A minimal solution exists only for the single, discrete value of $\nu_\lambda^\mu(\theta)$ that satisfies the constraints (A13) and (A14).

One can use the theory of continued fractions to find the minimal solution to the recurrence relation and determine $\nu_\lambda^\mu(\theta)$. Divide (A8) by $a_r(\theta)$ and consider the infinite continued fraction $P_{\lambda,r}^\mu(\theta)$ defined for $r \geq 1$ as

$$P_{\lambda,r}^\mu(\theta) \equiv \frac{a_r}{a_{r-1}} = \frac{-\mathcal{A}_r}{\mathcal{B}_r + \mathcal{C}_r \dfrac{a_{r+1}}{a_r}} = \cfrac{-\mathcal{A}_r}{\mathcal{B}_r + \mathcal{C}_r \cfrac{-\mathcal{A}_{r+1}}{\mathcal{B}_{r+1} + \mathcal{C}_{r+1} \cfrac{-\mathcal{A}_{r+2}}{\mathcal{B}_{r+2} + \ldots}}} \quad r \geq 1, \tag{A23}$$

where we have again suppressed for clarity the indices μ and λ as well as the argument θ. For a given choice of parameters μ, λ, θ, and ν the infinite continued fraction can be used to find the ratios a_r/a_{r-1} of all the expansion coefficients, for $r \geq 1$, *if the continued fraction converges*. There is no loss of generality if one assumes $a_0 = 1$ [19,20], (note that this is compensated for in the normalization $s_\lambda^\mu(\theta)$) so the continued fraction (if it converges) can be used to find the expansion coefficients a_r for $r \geq 1$.

A second infinite continued fraction for $r \leq -1$ can also be derived from the recurrence relation. We define the continued fraction

$$N_{\lambda,r}^\mu(\theta) \equiv \frac{a_r}{a_{r+1}} = \frac{-\mathcal{C}_r}{\mathcal{B}_r + \mathcal{A}_r \dfrac{a_{r-1}}{a_r}} = \cfrac{-\mathcal{C}_r}{\mathcal{B}_r + \mathcal{A}_r \cfrac{-\mathcal{C}_{r-1}}{\mathcal{B}_{r-1} + \mathcal{A}_{r-1} \cfrac{-\mathcal{C}_{r-2}}{\mathcal{B}_{r-2} + \ldots}}} \quad r \leq -1. \tag{A24}$$

Assuming $a_0 = 1$, the continued fraction (if it converges) can be used to find the expansion coefficients a_r for $r \leq -1$.

Whether or not the infinite continued fractions converge depends on the existence of minimal solutions to the recurrence relation. Pincherle's Theorem [24] tells us that the infinite continued fraction $P_\lambda^\mu(\theta)$ converges for $r \geq 1$ if and only if the recurrence relation has a *minimal* solution for $r \geq 1$. Further, if the infinite continued fraction does converge, it converges to a minimal solution. Likewise, $N_\lambda^\mu(\theta)$ converges to a minimal solution for $r \leq -1$ if and only if the recurrence relation has a minimal solution for $r \leq -1$.

A subtle, but important, point is that $P_\lambda^\mu(\theta)$ and $N_\lambda^\mu(\theta)$ may converge *to different minimal solutions*. Given a set of parameters μ, λ, θ and ν, the continued fraction (A23) (with $a_0 = 1$) may converge and determine a set of coefficients $a_1, a_2, a_3, \ldots$. These coefficients will satisfy the recurrence relation for $r \geq 1$ and will fall off for large r. Likewise, for the same set of parameters, the continued fraction (A24) may converge and determine a set of coefficients $a_{-1}, a_{-2}, a_{-3}, \ldots$, which will satisfy the recurrence relation for $r \leq -1$ and will fall of for large $|r|$. The recurrence relation for $r = 0$, however, *may not be satisfied*. This is because the $r = 0$ recurrence relation

$$\mathcal{A}_{\lambda,0}^\mu(\theta) a_{\lambda,-1}^\mu(\theta) + \mathcal{B}_{\lambda,0}^\mu(\theta) a_{\lambda,0}^\mu(\theta) + \mathcal{C}_{\lambda,0}^\mu(\theta) a_{\lambda,1}^\mu(\theta) = 0 \tag{A25}$$

is not explicitly solved when calculating either the $P_\lambda^\mu(\theta)$ or the $N_\lambda^\mu(\theta)$. One can see this by examining the continued fractions (A23) and (A24); the three coefficients a_{-1}, a_0, and a_1 do not appear together anywhere in (A23) and (A24) for any r. So both the set of expansion

coefficients $a_1, a_2, a_3, \ldots$ found using $P^\mu_\lambda(\theta)$ and the set $a_{-1}, a_{-2}, a_{-3}, \ldots$ found using $N^\mu_\lambda(\theta)$ are minimal solutions for a certain range of the index r, but not for all r.

In order for the recurrence relation (A8) to be satisfied it must be true for *all* r. To ensure this, one must match the two solutions found using the continued fractions. This is accomplished by requiring that

$$\mathcal{A}^\mu_{\lambda,0}(\theta) N^\mu_{\lambda,-1}(\theta) + \mathcal{B}^\mu_{\lambda,0}(\theta) + \mathcal{C}^\mu_{\lambda,0}(\theta) P^\mu_{\lambda,1}(\theta) \equiv Z^\mu_\lambda(\theta,\nu) = 0, \tag{A26}$$

which is just the requirement that the recurrence relation be satisfied for $r = 0$. So finding the minimal solution to the recurrence relation, and hence the characteristic exponent $\nu^\mu_\lambda(\theta)$, is equivalent to finding the root of the the function $Z^\mu_\lambda(\theta,\nu)$ defined in (A26). Given a test value for $\nu^\mu_\lambda(\theta)$, one calculates the continued fractions $P^\mu_{\lambda,1}(\theta)$ and $N^\mu_{\lambda,-1}(\theta)$, and the rational functions $\mathcal{A}^\mu_{\lambda,0}, \mathcal{B}^\mu_{\lambda,0}$, and $\mathcal{C}^\mu_{\lambda,0}$, to find $Z^\mu_\lambda(\theta,\nu)$. If Z^μ_λ is not zero, one modifies the test value for $\nu^\mu_\lambda(\theta)$ using whichever root-finding algorithm one prefers.

In practice, this method for determining $\nu^\mu_\lambda(\theta)$ is efficient. Figure 4 shows the function $Z^1_2(\theta,\nu)$ (of interest for the cosmological case) for $\theta = 5$ and $\frac{1}{2} < \nu < \frac{3}{2}$. This plot is typical for θ in the range $10^{-4} \le \theta \le 10^4$; the root $\nu^\mu_\lambda(\theta)$ is always located between two singularities, and Z^1_2 is positive for $\nu = \nu^\mu_\lambda(\theta) - \epsilon$ and negative for $\nu = \nu^\mu_\lambda(\theta) + \epsilon$ where $0 < \epsilon \ll 1$. This assists implementing a root-finding algorithm to find the zeroes of $Z^1_2(\theta,\nu)$ for arbitrary θ. Figure 5 shows the characteristic exponent $\nu^1_2(\theta)$ for $10^{-3} \le \theta \le 10^3$.

Once the characteristic exponent $\nu^\mu_\lambda(\theta)$ is determined, one can use the continued fractions (A23) and (A24), along with $a^\mu_{\lambda,0} = 1$ to calculate the remaining expansion coefficients. Since these coefficients are the minimal solution, the coefficients fall off for large $|r|$. One can then use (A10) to find $s^\mu_\lambda(\theta)$. Using (A4) and (A5), along with an algorithm for computing Bessel and Hankel functions, one can evaluate the spheroidal wave functions. Further details of the numerical techniques used may be found in Appendix B. Figure 6 shows the spheroidal wave functions ${}^1\mathsf{S}^1_2(z,\theta)$ and ${}^2\mathsf{S}^1_2(z,\theta)$ as functions of z for two values of θ.

APPENDIX B

This appendix briefly describes the numerical techniques used to obtain the results in section V B. One may separate the problem of numerically evaluating the spheroidal wave functions ${}^1\mathsf{S}^1_2(z,\theta)$ and ${}^2\mathsf{S}^1_2(z,\theta)$ into two parts. The first is to determine the characteristic exponent $\nu^1_2(\theta)$ for a given θ. As noted in section A 6 the characteristic exponent $\nu^1_2(\theta)$ is that value of ν for which the function $Z^1_2(\theta,\nu)$ vanishes, where

$$Z^1_2(\theta,\nu) \equiv \mathcal{A}^1_{2,0}(\theta) N^1_{2,-1}(\theta) + \mathcal{B}^1_{2,0}(\theta) + \mathcal{C}^1_{2,0}(\theta) P^1_{2,1}(\theta). \tag{B1}$$

To find the root of $Z^1_2(\theta,\nu)$ (and hence the characteristic exponent $\nu^1_2(\theta)$) one must evaluate the five functions on the right-hand side of (B1). From (A9) one can see that the three functions $\mathcal{A}^1_{2,0}, \mathcal{B}^1_{2,0}$, and $\mathcal{C}^1_{2,0}$ (here $\lambda = 2$, *not* ν) are rational functions of ν for any θ, and are easily evaluated. The continued fractions $N^1_{2,-1}(\theta)$ and $P^1_{2,1}(\theta)$, defined by (A23) and (A24), are evaluated using the modified Lentz's method (see section 5.2 in reference [25]). Both continued fractions usually converge within 10 iterations when evaluated using this method. The root of $Z^1_2(\theta,\nu)$ is found using a simple bisection method. Although bisection may not be as efficient as other methods, it has the advantage that it is guaranteed to work once the

root has been bracketed. This is helpful since we are interested in finding the root $\nu_2^1(\theta)$ of $Z_2^1(\theta,\nu)$ for many different θ; for some θ the root $\nu_2^1(\theta)$ lies *very* close to a singularity of $Z_2^1(\theta,\nu)$, and in these cases other root-finding methods may not converge (see section 9.2 in reference [25]).

Once the characteristic exponent $\nu_2^1(\theta)$ has been calculated, the remaining problem is to calculate the sums (A20) of expansion coefficients $a_{2,r}^1(\theta)$ times Bessel functions $J_{\nu+2r+1/2}(2\theta^{1/2}z)$ and $Y_{\nu+2r+1/2}(2\theta^{1/2}z)$. The expansion coefficients are calculated using the continued fractions $N_{2,r}^1(\theta)$ and $P_{2,r}^1(\theta)$. With $a_{2,0}^1(\theta)=1$, one has $a_{2,1}^1(\theta)=P_{2,1}^1(\theta)$, $a_{2,2}^1(\theta)=P_{2,2}^1(\theta)P_{2,1}^1(\theta)$, and in general

$$a_{2,n}^1(\theta)=\prod_{j=1}^{n}P_{2,j}^1(\theta). \tag{B2}$$

Likewise, the negative index expansion coefficients are given by

$$a_{2,-n}^1(\theta)=\prod_{j=1}^{n}N_{2,-j}^1(\theta). \tag{B3}$$

The continued fractions $N_{2,r}^1(\theta)$ and $P_{2,r}^1(\theta)$ are calculated using the modified Lentz's method as noted above. The normalization $s_2^1(\theta)$, defined in (A10), is calculated at the same time as the expansion coefficients.

The Bessel functions are calculated most efficiently using recurrence relations. The functions $J_{\nu+2r+1/2}(2\theta^{1/2}z)$ and $Y_{\nu+2r+1/2}(2\theta^{1/2}z)$ with $r\geq 0$ and $r<0$ are handled separately. For $r\geq 0$, $J_{\nu+2r+1/2}(2\theta^{1/2}z)$ and $J_{\nu+2r+1/2-2}(2\theta^{1/2}z)$ are calculated for some large r using the routine bessjy() found in reference [25]. Using the recurrence relations for Bessel functions (see 3.87 and 3.88 in [15]), the $J_{\nu+2r+1/2}(2\theta^{1/2}z)$ are calculated using downward recursion to $r=0$ (this is the direction in which the recursion is stable for Bessel functions of the first kind [25]). A similar procedure, using upward recursion, is used for the Bessel functions of the second kind $Y_{\nu+2r+1/2}(2\theta^{1/2}z)$. This gives the necessary Bessel functions for $r\geq 0$.

The reflection formulae for Bessel functions are used to calculate the Bessel functions for $r<0$. Since the index

$$\nu+2r+1/2=-(2|r|-\nu-1/2)\ \text{ for }\ r<0\ \text{ and }\ 1/2<\nu<3/2, \tag{B4}$$

the same procedure outlined above is used for $J_{2|r|-\nu-1/2}(2\theta^{1/2}z)$ and $Y_{2|r|-\nu-1/2}(2\theta^{1/2}z)$, and then the reflection formulae (see 6.7.19 of [25])

$$J_{-\upsilon}(y)=\cos\upsilon\pi J_\upsilon(y)-\sin\upsilon\pi Y_\upsilon(y), \tag{B5}$$

$$Y_{-\upsilon}(y)=\sin\upsilon\pi J_\upsilon(y)+\cos\upsilon\pi Y_\upsilon(y), \tag{B6}$$

are used to find $J_{\nu+2r+1/2}(2\theta^{1/2}z)$ and $Y_{\nu+2r+1/2}(2\theta^{1/2}z)$ for $r<0$. So all the Bessel functions needed are calculated with only a few time-consuming calls to the routine bessjy().

Once the expansion coefficients $a_{2,r}^1(\theta)$ and the Bessel functions $J_{\nu+2r+1/2}(2\theta^{1/2}z)$ and $Y_{\nu+2r+1/2}(2\theta^{1/2}z)$ are tabulated, the sums in (A20) are calculated. Care must be taken when terminating the sums. Although the expansion coefficients $a_{2,r}^1(\theta)$ fall off *very* quickly as $|r|$ becomes large, the products $a_{2,r}^1(\theta)J_{\nu+2r+1/2}(2\theta^{1/2}z)$ and $a_{2,r}^1(\theta)Y_{\nu+2r+1/2}(2\theta^{1/2}z)$ may not

fall off as fast. We terminate the sums when the *products* of the expansion coefficients and Bessel functions no longer contribute (at double-precision accuracy) to the sums.

The primary numerical technique used to evaluate the multipole moments (5.2) is numerical integration. Both the integral over κ in (5.2) and the integral over x in (5.3) were done using a fifth order embedded Runge-Kutta-Fehlberg algorithm with adaptive stepsize control [25]. Although formally the upper limit of the integral over κ extends to infinity, we only integrated until the remaining contribution became negligible. The Bessel function with index $l + 1/2$ was evaluated with the routine bessjy().

REFERENCES

[1] R. K. Sachs and A. M. Wolfe, Astrophys. J. **147**, 73 (1967).

[2] Bruce Allen and Scott Koranda, Phys. Rev. D **50**, 3713 (1994). Note that the caption for Table I of this reference should indicate that the multipoles listed in the table have been divided by $\rho_{\rm ds}/\rho_{\rm P}$. Also note that the definition of M_l given in the caption of Figure 2 contains a spurious factor of $\rho_{\rm ds}/\rho_{\rm p}$; the correct definition is given by (5.5) of this paper.

[3] V.A. Rubakov, M.V. Sazhin and A.V. Veryaskin, Phys. Lett. **115B**, 189 (1982) .

[4] R. Fabbri and M.D. Pollock, Phys. Lett. **125B**, 445 (1983).

[5] L.F. Abbott and M.B. Wise Nucl. Phys. **B244**, 541 (1984) ; Phys. Lett. **135B**, 279 (1984).

[6] A. A. Starobinsky, Pis'ma Astron. Zh. **9**, 579 (1983) [Sov. Astron. Lett. **9**, 302 (1983)]; Pis'ma Astron. Zh. **11**, 323 (1985) [Sov. Astron. Lett. **11**, 133 (1985)].

[7] M. White, Phys. Rev. D **46**, 4198 (1992).

[8] L.P. Grishchuk, Phys. Rev. Lett. **70**, 2371 (1993) ; Class. Quantum Grav. **10**, 2449 (1993) ; Phys. Rev. D **48**, 3513 (1993) ; Phys. Rev. D **48**, 5581 (1993) ; Phys. Rev. D **46**, 1440 (1992).

[9] Michael S. Turner, Martin White, and James E. Lidsey, Phys. Rev. D **48**, 4613 (1993).

[10] K. Ng and A.D. Speliotopoulos, *Cosmological Evolution of Scale-Invariant Gravity Waves*, Institute of Physics, Academia Sinica, Taiwan preprint **IP-ASTP-07-94** (May 1994).

[11] Robert Crittenden, J. Richard Bond, Richard L. Davis, George Efstathiou, and Paul J. Steinhardt, Phys. Rev. Lett. **71**, 324 (1993).

[12] Scott Dodelson, Lloyd Knox, and Edward W. Kolb, Phys. Rev. Lett. **72**, 3444 (1994).

[13] V. Sahni, Phys. Rev. D **42**, 453 (1990); Class. Quantum Grav. **5**, L113 (1988).

[14] H. Nariai, Suppl. Prog. Theor. Phys. **70**, 301 (1981).

[15] J. D. Jackson, *Classical Electrodynamics* (Wiley, New York, 1975).

[16] For a review of inflationary cosmology see E. Kolb and M. Turner, *The Early Universe*, (Addison-Wesley, New York, 1990).

[17] B. Allen, Phys. Rev. D. **37**, 2078 (1988).

[18] L.H. Ford and Leonard Parker, Phys. Rev. D **16**, 245 (1977) ; **16**, 1601 (1977).

[19] *Higher Transcendental Functions*, edited by A. Erdélyi (Robert E. Krieger Publishing, Malabar, Florida, 1981), vol 3.

[20] J. Meixner and F. W. Schäfke, *Mathieusche Funktionen und Sphäroidfunktionen, mit Anwendungen auf physikalische und technische Probleme* (Springer, Berlin, 1954).

[21] *Handbook of Mathematical Functions*, Natl. Bur. Stand. Appl. Math. Ser. No. 55, edited by M. Abramowitz and I. Stegun (U.S. GPO, Washington, D.C., 1972).

[22] C. Flammer, *Spheroidal Wave Functions* (Stanford University Press, Stanford, CA, 1957); J.A. Stratton, et. al., *Spheroidal Wave Functions, including Tables of Separation Constants and Coefficients* (published jointly by The Technology Press of M.I.T. and Wiley and Sons, New York, 1956).

[23] P.M. Morse and H. Feshbach, *Methods of Theoretical Physics* (McGraw-Hill, New York, 1953).

[24] W. Gautschi, SIAM Review, **9**, 24 (1967).

[25] William H. Press, et. al., *Numerical Recipes in C*, 2nd ed. (Cambridge University Press, Cambridge, 1992).

FIGURES

FIG. 1. Multipole moments $\langle a_l^2 \rangle$ normalized to the quadrupole $\langle a_2^2 \rangle$. The horizontal axis is the index l of the multipole moment and the vertical axis is M_l. See (5.5) for the definition of M_l. The points labeled "mixed" show results obtained from the (5.2) and (5.3) which analytically model a universe containing both dust and radiation, and which is not completely dust dominated at last-scattering. The points labeled "transfer function" show results from Turner, White, and Lidsey [9] obtained using a transfer function.

FIG. 2. Multipole moments $\langle a_l^2 \rangle$ normalized to the quadrupole $\langle a_2^2 \rangle$. The axes are the same as in Figure 1. The points labeled "mixed" show results obtained from (5.2) and (5.3) which analytically model a universe containing both dust and radiation, and which is not completely dust dominated at last-scattering. The points labeled "exact-dust" show results obtained using Eq. (6.2) of Allen and Koranda [2]. The points labeled "approximate-dust" shows results obtained by evaluating Eq. (6.1) (which is a long-wavelength approximation to Eq. (6.2)) of Allen and Koranda [2]. Both sets of points "exact-dust" and "approximate-dust" are for universe models that are *completely* dust dominated at last-scattering.

FIG. 3. Multipole moments $\langle a_l^2 \rangle$ normalized to the quadrupole $\langle a_2^2 \rangle$. The axes are the same as in Figure 1. The points labeled "mixed" show results obtained from (5.2) and (5.3) which analytically model a universe containing both dust and radiation, and which is not completely dust dominated at last-scattering. The points labeled "Boltzmann" show results from Dodelson, Knox, and Kolb [12], who do not use the Sachs-Wolfe formula to calculate the CBR anisotropy. Instead they use numerical methods to evolve the photon distribution function using first-order perturbation theory of the general relativistic Boltzmann equation for radiative transfer.

FIG. 4. The function $Z_2^1(\theta, \nu)$ plotted versus ν for $\theta = 5$. The value of ν at which this function vanishes is the characteristic exponent $\nu_2^1(\theta)$ for $\theta = 5$. This plot is typical for values of θ in the range $10^{-4} \leq \theta \leq 10^4$. The root is always located between two singularities.

FIG. 5. The characteristic exponent $\nu_2^1(\theta)$ plotted vs $\log \theta$. Only for certain discrete values of θ is ν equal to 1. For this reason the function $S_1^{1(j)}(z, \theta)$ is not a valid solution to the differential equation (A1) for $\mu = 1, \lambda = 2$, and θ arbitrary.

FIG. 6. The spheroidal wave functions ${}^1\mathsf{S}_2^1(z, \theta)$ (solid lines) and ${}^2\mathsf{S}_2^1(z, \theta)$ (dotted lines) for $\theta = 0.1$ and $\theta = 10$. Both functions diverge in the limit as $z \to 1$. Note that the vertical scales are different for the two plots.

TABLES

TABLE I. List of free parameters that define the cosmological model

Parameter	Units	Range	Description
H_0	length^{-1}	$H_0 > 0$	Present-day Hubble expansion rate
$Z_{\rm ls}$	dimensionless	$Z_{\rm ls} > 0$	Redshift at last scattering of CBR
$Z_{\rm eq}$	dimensionless	unrestricted	Redshift at equal matter/radiation energy density
$Z_{\rm end}$	dimensionless	$Z_{\rm end} > Z_{\rm eq}, Z_{\rm ls}$	Redshift at end of de Sitter inflation

TABLE II. Multipole moments $\langle a_l^2 \rangle$ evaluated using different methods. These have been divided by the scale of the moments $\rho_{\rm ds}/\rho_{\rm p}$. The second column shows multipoles for a mixed cosmology obtained from the formulae (5.2) and (5.3), which analytically model a universe containing both dust and radiation, and which is not completely dust dominated at last-scattering. The third column shows results obtained by evaluating Eq. (6.2) of Allen and Koranda [2], which assumes that the universe was completely dust dominated at last-scattering. The fourth column shows results obtained by evaluating Eq. (6.1) of Allen and Koranda, which is a long wavelength approximation to their Eq. (6.2), and equivalent to standard formula of Abbott and Wise [5] and Starobinsky [6]. The fifth column shows results obtained by Ng and Speliotopoulos [10], who numerically integrated the wave equation to obtain the amplitude of the gravitational waves. They also considered a universe model which is not completely dust dominated at last-scattering. All the results were obtained with $Z_{\rm eq} = 6000$ and $Z_{\rm ls} = 1100$.

l	$\langle a_l^2 \rangle \frac{\rho_{\rm P}}{\rho_{\rm dS}}$ this work Eq. (5.2)	$\langle a_l^2 \rangle \frac{\rho_{\rm P}}{\rho_{\rm dS}}$ Allen, Koranda Eq. (6.2) of ref. [2]	$\langle a_l^2 \rangle \frac{\rho_{\rm P}}{\rho_{\rm dS}}$ Allen, Koranda Eq. (6.1) of ref. [2]	$\langle a_l^2 \rangle \frac{\rho_{\rm P}}{\rho_{\rm dS}}$ Ng, Speliotopoulos Table 1 of ref. [10]
2	1.54	1.52	1.52	1.55
3	6.07×10^{-1}	6.07×10^{-1}	6.07×10^{-1}	
4	3.44×10^{-1}	3.44×10^{-1}	3.44×10^{-1}	
5	2.27×10^{-1}	2.27×10^{-1}	2.27×10^{-1}	
6	1.63×10^{-1}	1.62×10^{-1}	1.62×10^{-1}	
7	1.23×10^{-1}	1.22×10^{-1}	1.22×10^{-1}	
8	9.66×10^{-2}	9.61×10^{-2}	9.58×10^{-2}	
9	7.80×10^{-2}	7.74×10^{-2}	7.71×10^{-2}	
10	6.43×10^{-2}	6.37×10^{-2}	6.34×10^{-2}	
20	1.74×10^{-2}	1.69×10^{-2}	1.66×10^{-2}	1.75×10^{-2}
50	2.36×10^{-3}	1.99×10^{-3}	1.83×10^{-3}	2.36×10^{-3}
100	1.91×10^{-4}	8.67×10^{-5}	6.23×10^{-5}	1.90×10^{-4}
150	7.45×10^{-6}	4.11×10^{-6}	1.89×10^{-6}	7.41×10^{-6}
200	4.56×10^{-6}	3.68×10^{-6}	9.96×10^{-7}	4.49×10^{-6}

Figure 1

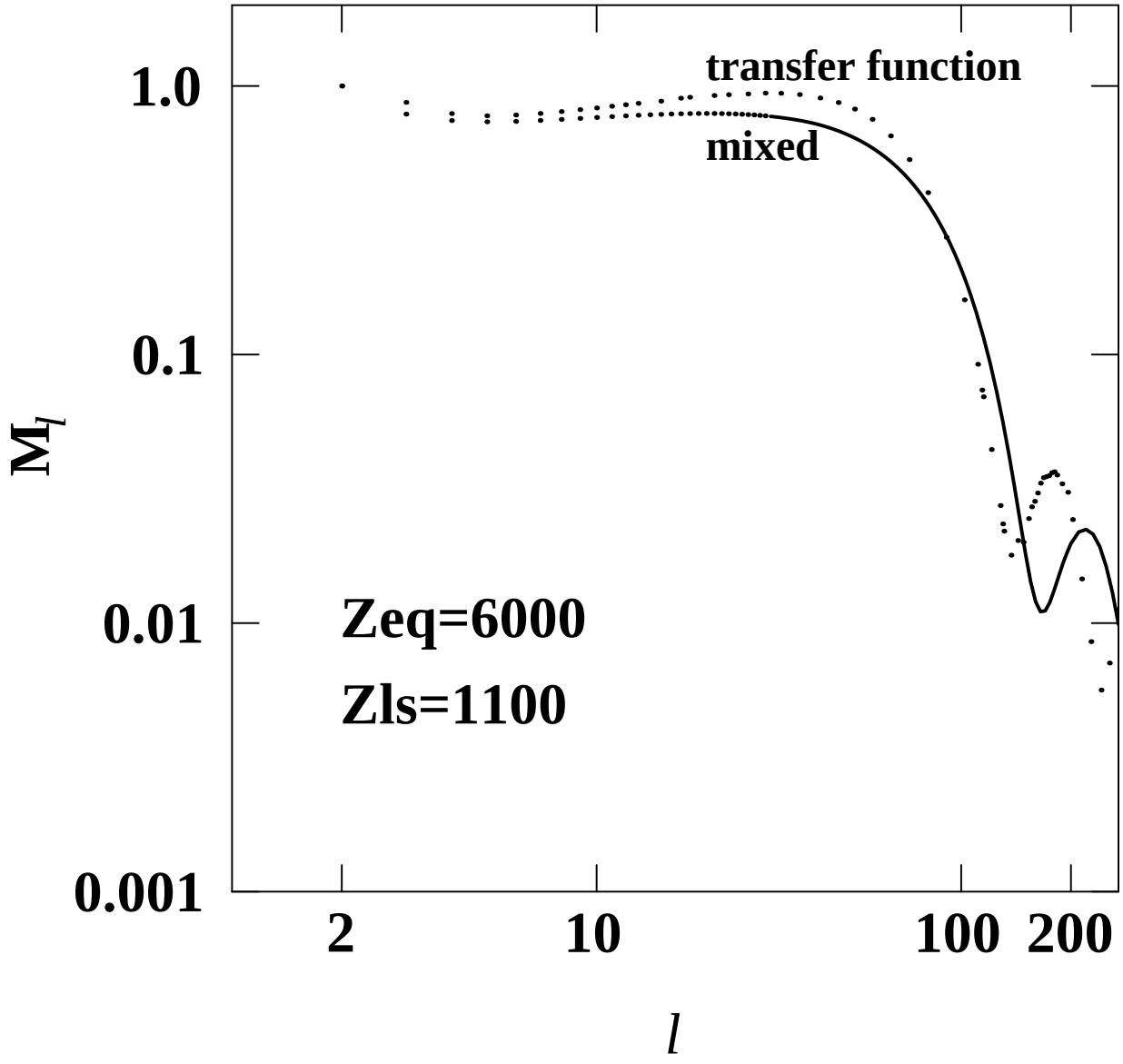
transfer function
mixed
1.0
0.1
0.01
0.001
M_l
Zeq=6000
Zls=1100
2
10
100
200
l

This figure "fig1-1.png" is available in "png" format from:

http://arXiv.org/ps/astro-ph/9410049v3

Figure 2

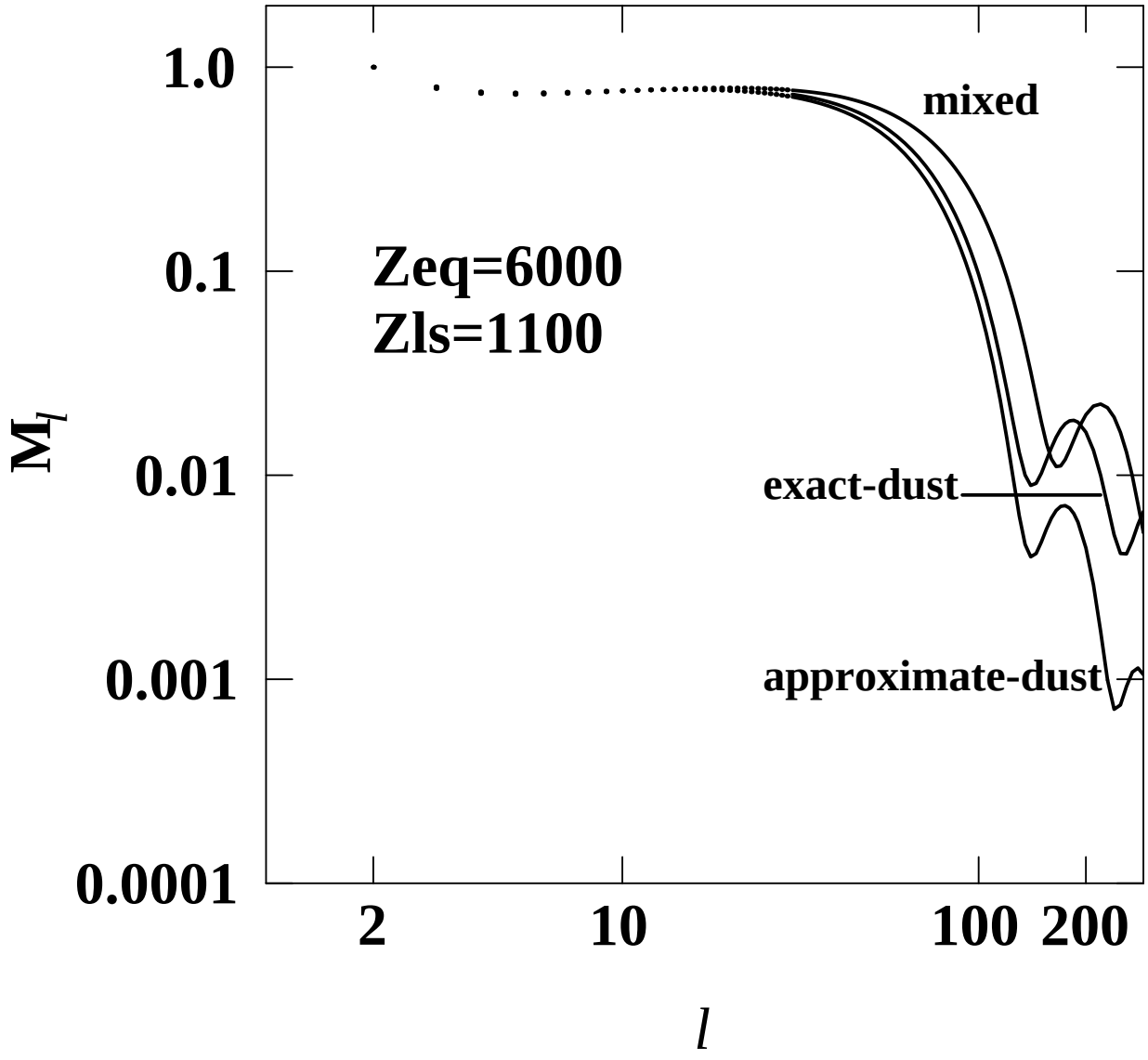
1.0
0.1
0.01
0.001
0.0001
M_l
Zeq=6000
Zls=1100
mixed
exact-dust
approximate-dust
2
10
100
200
l

This figure "fig1-2.png" is available in "png" format from:

http://arXiv.org/ps/astro-ph/9410049v3

Figure 3

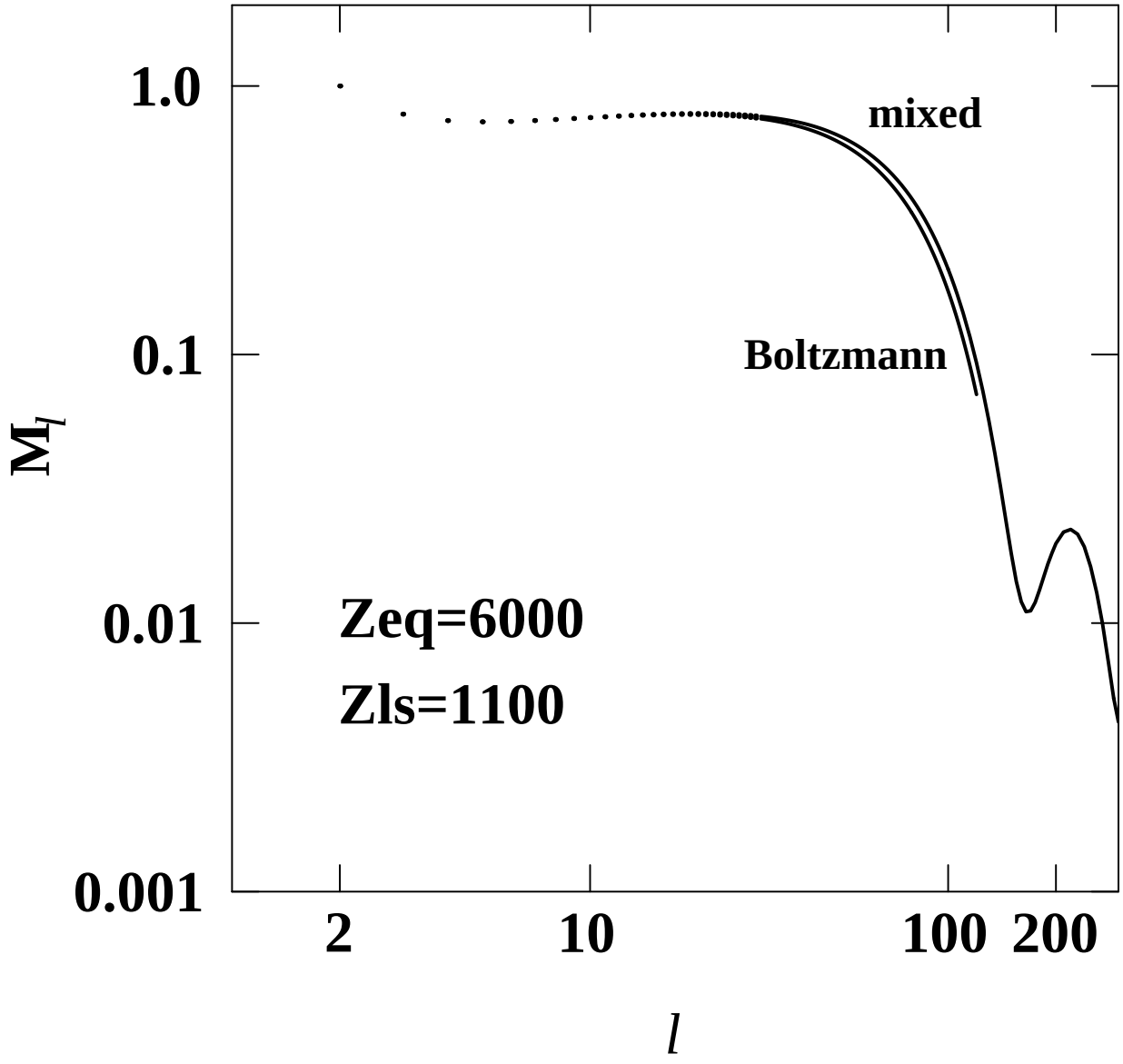
1.0
0.1
0.01
0.001
M_l
mixed
Boltzmann
Zeq=6000
Zls=1100
2
10
100
200
l

This figure "fig1-3.png" is available in "png" format from:

http://arXiv.org/ps/astro-ph/9410049v3

Figure 4

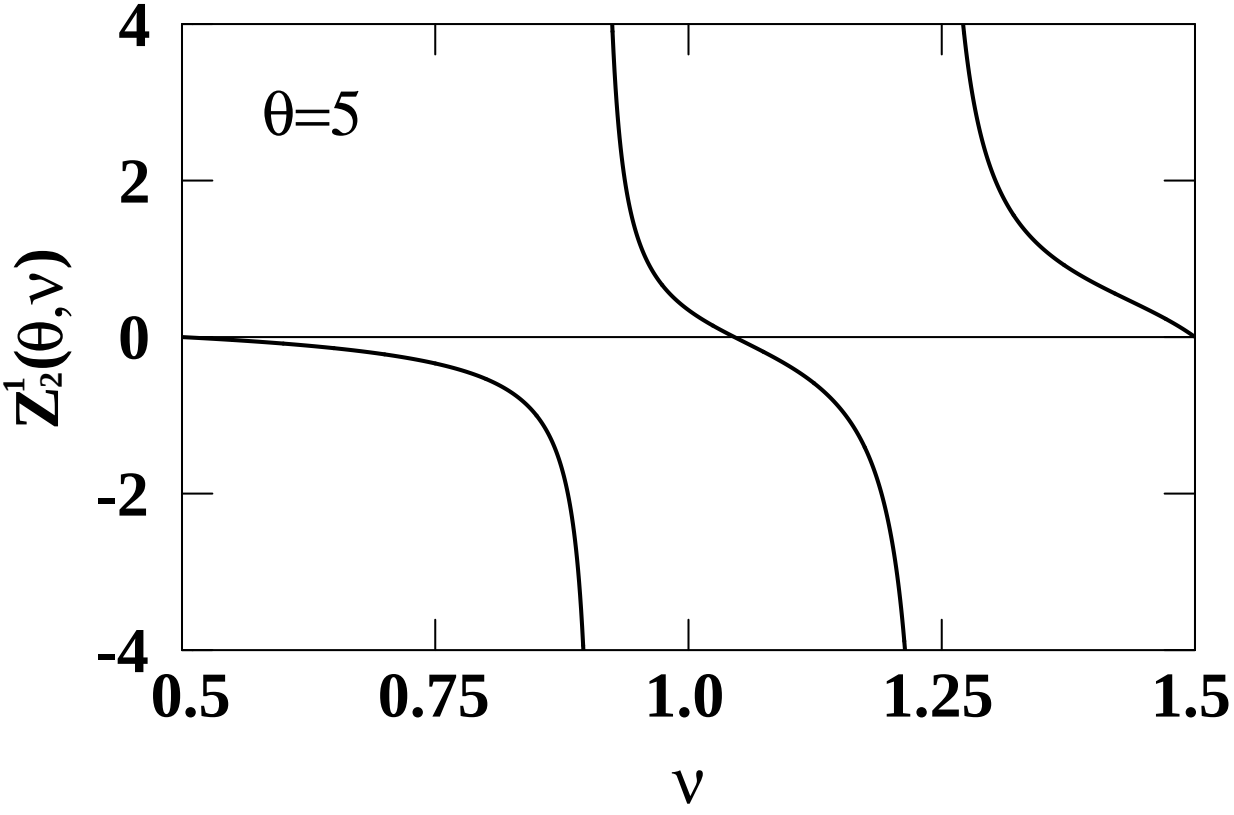

This figure "fig1-4.png" is available in "png" format from:

http://arXiv.org/ps/astro-ph/9410049v3

Figure 5

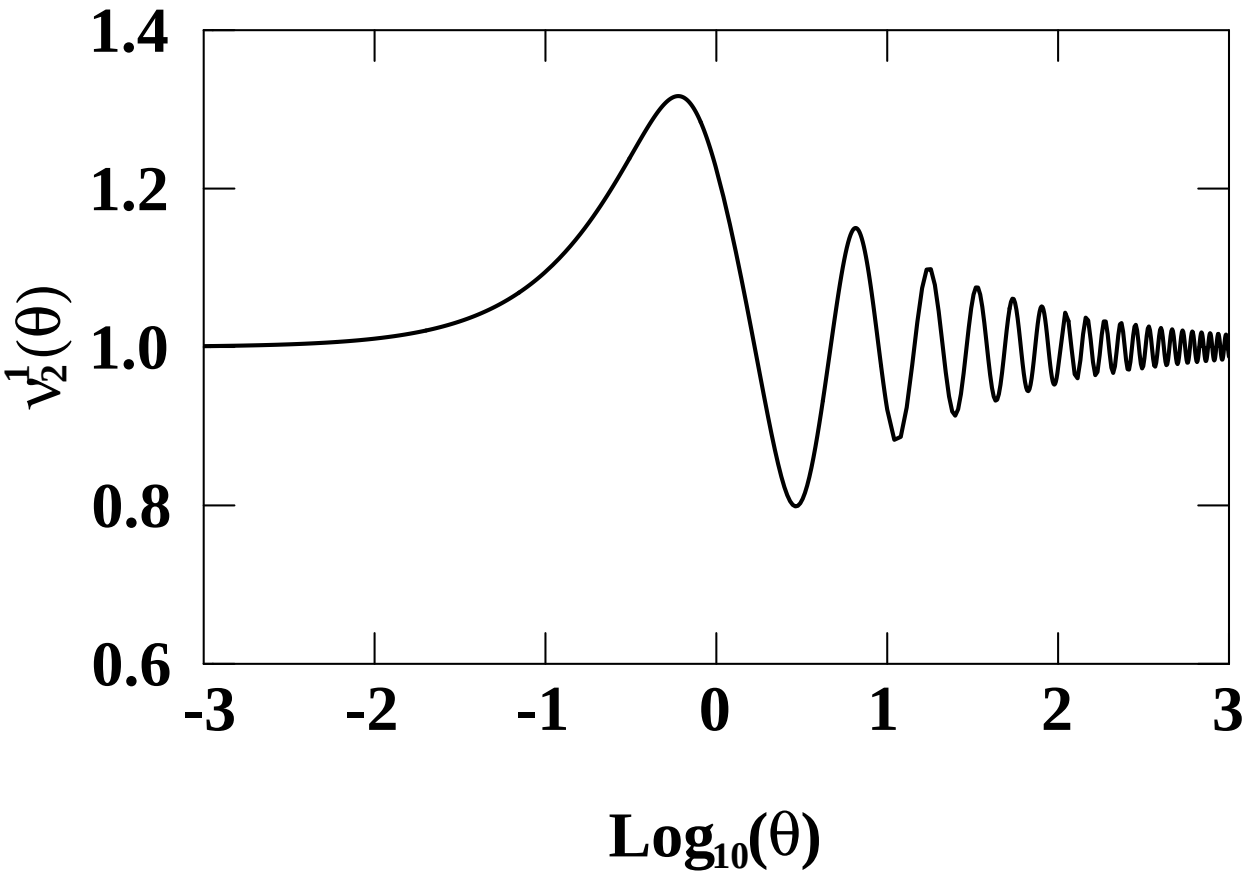

This figure "fig1-5.png" is available in "png" format from:

http://arXiv.org/ps/astro-ph/9410049v3

Figure 6

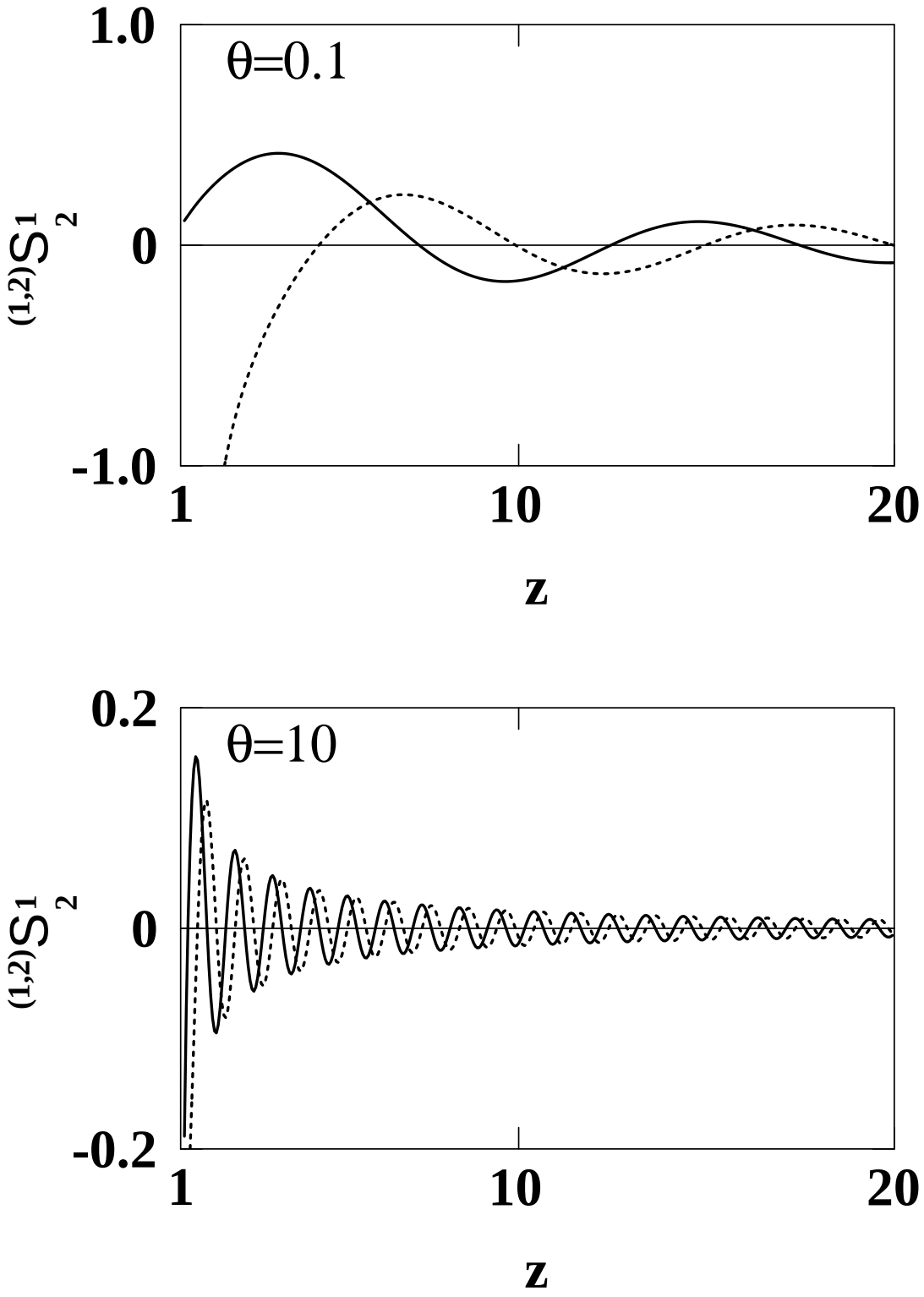

This figure "fig1-6.png" is available in "png" format from:

http://arXiv.org/ps/astro-ph/9410049v3